Positive-parity excited baryons in a quark model with hyperfine interactions

Nathan Isgur*
Department of Theoretical Physics, University of Oxford, 1 Keble Road, Oxford OX1 3NP, England

Gabriel Karl†
Theory Division, Rutherford Laboratory, Chilton, Didcot, Oxon OX11 OQX, England

(Received 11 August 1978)

A quark model suggested by quantum chromodynamics with strong spin-dependent forces of magnetic-dipole–magnetic-dipole character perturbing a flavor-independent confinement potential is applied to low-lying positive-parity excited baryons. SU(3) is broken only by quark masses, and this leads to a new choice of basis states in the hyperon sector; couplings to $\bar{K}N$ are especially transparent in this basis. The results, which are largely determined by previous analyses, are in good agreement with the known properties of these states. Spin-orbit forces are once again found to be negligible.

I. INTRODUCTION

This paper is one of a series[1,2,3] on baryons in the quark model and so it hardly needs a separate introduction. We shall just comment briefly on recent developments in quark models of "old" hadrons and then turn to the subject of this paper.

Most new work on quark models has been stimulated by the recognition of similarities between quark interactions and electromagnetism. In particular this has led to applications of hyperfine interactions to baryon[1-6] and meson[4,7,8] spectroscopy, and to various hadronic properties like the charge radius of the neutron.[9] Although it is too early to summarize it seems that hyperfine interactions (including their tensor component) are indeed helpful in understanding hadrons.

A simple example, indicative of recent insight, is provided by Σ, Λ splittings. In the ground-state ^2S-wave multiplet, Λ and Σ differ in the spin of the nonstrange-quark pair, and this leads to different hyperfine interactions between quarks: The $\Sigma\frac{1}{2}^+$-$\Lambda\frac{1}{2}^+$ mass difference can then be quantitatively understood as a consequence of the smaller color magnetic moment of the strange quark.[4] In excited P-wave baryons, for a given quark spin state the Σ and Λ will differ in the *orbital* motion of the quarks: The "reverse" ordering $\Lambda\frac{5}{2}^- > \Sigma\frac{5}{2}^-$ then arises as a consequence of the higher mass of the strange quark and the attendant lower frequency of the corresponding orbital mode.[2,3]

We have previously analyzed the negative-parity baryons in a very simple model[1,2,3] which contains only flavor-independent harmonic forces and hyperfine interactions between quarks. This model works very well for masses and mixing angles; furthermore, many features of the analysis appear to be independent of the use of harmonic forces. The purpose of the present investigation is to extend the quark model described previously to low-lying positive-parity excitations of the three-quark system.

There are many excited positive-parity orbital modes for a three-particle system.[10] These modes differ from each other in their orbital angular momentum L and their behavior under permutations. As is well known, each type of permutational behavior corresponds to an SU(6) multiplet (56;70;20) if forces between quarks are SU(6) invariant. Thus for harmonic forces between quarks one would expect five degenerate SU(6) multiplets at $N=2$: 56 ($L=0$ and 2), 70 ($L=0$ and 2), and 20 ($L=1$). These states are not, however, all found to be degenerate experimentally. There are two simple reasons for the departure from this ideal limit: Forces between quarks are not harmonic and, secondly, quark masses are not identical. Because forces between quarks are not harmonic different orbital modes become separated from each other in mass. This is discussed in the next section and in Appendix A. In addition to this SU(6)-invariant perturbation there is SU(6) breaking when we turn to hyperons. This is similar to the SU(3) breaking found in negative-parity hyperons,[2,3,6] and leads also in this case to a pattern of mixings which segregates those states which couple to the $\bar{K}N$ channel from those which do not. This will lead to effects which extend the proposal of Petersen and Rosner[11] and of Faiman[11] to positive-parity baryons. After taking into account these orbital effects, we consider the effects of the hyperfine interaction in Sec. III and Appendix C. The comparison with the experimental data is discussed in Sec. IV. A nice feature of this comparison is the good correlation between those states which are well observed in $\bar{K}N$ scattering and those which we predict to couple strongly to this channel: The mixing angles are therefore obtained satisfactorily. The mixings of hyperons are most transparent in a basis, previously introduced for negative-parity states,[2,3,6] in which the generalized Pauli principle is employed only for nonstrange quarks. On the other hand, for the nonstrange states, and even for many calculations involving strange states, a symmetrized basis is more convenient. As a result we tend to shuttle back and forth between these two bases which are defined and connected to each other in Appendix B. Finally our conclusions are discussed in Sec. V.

II. HAMILTONIAN AND ZEROTH-ORDER STATES

The states with which we are concerned here are those which are associated with the $N=2$ level of the harmonic-oscillator model, namely the states of the five SU(6) multiplets $(56', 0^+)$, $(70, 0^+)$, $(56, 2^+)$, $(70, 2^+)$, and $(20, 1^+)$. From the point of view of this calculation, however, the importance of the SU(6) symmetry is much diminished; while SU(6) remains a useful classification scheme it loses most of its dynamical significance. Of course in the limit that one turns off quark mass differences and hyperfine interactions, the states do all collapse into their appropriate degenerate SU(6) multiplets, and we shall find it useful to refer to this limit. In the nonstrange sector of positive-parity baryons, where SU(6) is broken only by hyperfine interactions, we have still found it convenient, in fact, to describe the states in terms of an essentially SU(6) basis. In the $S=-1$ sector, however, the SU(6) basis becomes inappropriate and we turn to a basis (which we call the *uds* basis) in which the strange quark is treated as distinguishable from the two nonstrange quarks. That such a basis is much more relevant for the strange baryons has already been made clear from our discussion of the negative-parity states.[2,3] We continue to find in our discussion of the $S=-1$ positive-parity states that the use of the *uds* basis considerably clarifies the physics.

As in our previous study of the negative-parity baryons we assume that the Hamiltonian for the baryons is of the form

$$H=\sum_i m_i + H_0 + H_{\text{hyp}}\,, \tag{1}$$

$$H_0=\sum_i \frac{p_i^{\,2}}{2m_i} + V_{\text{conf}}\,, \tag{2}$$

where V_{conf} is a confining potential which is assumed to be a flavor-independent function of the relative quark separation, and H_{hyp} is the hyperfine interaction given by

$$H_{\text{hyp}}=\sum_{i<j} H_{\text{hyp}}^{ij}\,, \tag{3}$$

$$H_{\text{hyp}}^{ij}=\frac{2\alpha_s}{3m_i m_j}\left\{\frac{8\pi}{3}\vec{S}_i\cdot\vec{S}_j\delta^3(\vec{r}_{ij}) + \frac{1}{r_{ij}^{\,3}}\left[\frac{3\vec{S}_i\cdot\vec{r}_{ij}\vec{S}_j\cdot\vec{r}_{ij}}{r_{ij}^{\,2}}-\vec{S}_i\cdot\vec{S}_j\right]\right\}. \tag{4}$$

The second term in (4) is called the tensor term H_{tensor}^{ij} and is the interaction of one color magnet with the external dipole field of the other. The first term is called the contact term H_{contact}^{ij}; it may be visualized as arising from the interaction of one dipole with the color magnetic field internal to the other.

In our analysis of the negative-parity baryons we were able to simply take V_{conf} to be harmonic; for the present problem this approximation is no longer adequate. The negative-parity P-wave baryons are all contained in a single SU(6) multiplet (a 70-plet). On the other hand, the positive-parity excited baryons are to be found in five distinct SU(6) multiplets (as will be discussed in what follows), and while V_{conf} will give all the states of a given multiplet the same energy, the energies of different multiplets will, in general, be different. The harmonic-oscillator model, on the other hand, would make all five multiplets degenerate with energy $2\hbar\omega$ above the ground state. The experimental spectrum does not have this degeneracy, indicating that the spin-independent forces are not harmonic; as a result this useful approximation must be abandoned. This situation should not be surprising, especially within the context of QCD. After all, even if the "true" confining potential were harmonic, into what is here called V_{conf} we have lumped terms from the one-gluon-exchange potential such as the Coulomb-type interaction. There is of course no reason as well to assume that the "true" confining potential is harmonic; a linear potential would be a much more popular choice (although for the relative separations relevant here, a linear potential would be a choice that is, in our opinion, no more plausible). The harmonic-oscillator states are nevertheless a convenient set of base states for our discussion, and so we shall write

$$V_{\text{conf}}=\sum_{i<j} V_{\text{conf}}^{ij}\,, \tag{5}$$

$$V_{\text{conf}}^{ij}=\tfrac{1}{2}Kr_{ij}^{\,2}+U(r_{ij})\,, \tag{6}$$

where $U(r_{ij})$ is unknown. It is of course clear that we will no longer be able to obtain exact solutions for the zeroth-order eigenstates of V_{conf}, unlike the situation in the negative-parity baryons. Nevertheless, with a few plausible assumptions we can obtain a satisfactory description of the zeroth-order states.

A. The $S = 0$ sector

We begin by discussing the solutions to the harmonic-oscillator problem with

$$m_1 = m_2 = m_3 = m \tag{7}$$

as is appropriate to this sector. In this case H_0 becomes

$$H_0 = \frac{p_\lambda^2}{2m} + \frac{p_\rho^2}{2m} + \frac{3K}{2}(\rho^2 + \lambda^2), \tag{8}$$

where

$$\vec{\rho} \equiv \frac{1}{\sqrt{2}}(\vec{r}_1 - \vec{r}_2), \quad \vec{p}_\rho \equiv m\frac{d\vec{\rho}}{dt}, \tag{9}$$

$$\vec{\lambda} \equiv \frac{1}{\sqrt{6}}(\vec{r}_1 + \vec{r}_2 - 2\vec{r}_3), \quad \vec{p}_\lambda \equiv m\frac{d\vec{\lambda}}{dt}, \tag{10}$$

and the eigenstates of the Hamiltonian which lie $2\hbar\omega$ above the ground state (i.e., with $N = 2$) can be chosen to be

$$\psi_{00}^{S'} \equiv \frac{1}{\sqrt{3}}\frac{\alpha^5}{\pi^{3/2}}(\rho^2 + \lambda^2 - 3\alpha^{-2}) \exp[-\tfrac{1}{2}\alpha^2(\rho^2 + \lambda^2)], \tag{11}$$

$$\psi_{00}^{\rho} \equiv \frac{2}{\sqrt{3}}\frac{\alpha^5}{\pi^{3/2}}\vec{\rho}\cdot\vec{\lambda} \exp[-\tfrac{1}{2}\alpha^2(\rho^2 + \lambda^2)], \tag{12}$$

$$\psi_{00}^{\lambda} \equiv \frac{1}{\sqrt{3}}\frac{\alpha^5}{\pi^{3/2}}(\rho^2 - \lambda^2) \exp[-\tfrac{1}{2}\alpha^2(\rho^2 + \lambda^2)], \tag{13}$$

$$\psi_{22}^{S} \equiv \frac{1}{2}\frac{\alpha^5}{\pi^{3/2}}(\rho_+^2 + \lambda_+^2) \exp[-\tfrac{1}{2}\alpha^2(\rho^2 + \lambda^2)], \tag{14}$$

$$\psi_{22}^{\rho} \equiv \frac{\alpha^5}{\pi^{3/2}}\rho_+\lambda_+ \exp[-\alpha^2(\rho^2 + \lambda^2)], \tag{15}$$

$$\psi_{22}^{\lambda} \equiv \frac{1}{2}\frac{\alpha^5}{\pi^{3/2}}(\rho_+^2 - \lambda_+^2) \exp[-\tfrac{1}{2}\alpha^2(\rho^2 + \lambda^2)], \tag{16}$$

$$\psi_{11}^{A} \equiv \frac{\alpha^5}{\pi^{3/2}}(\rho_+\lambda_3 - \rho_3\lambda_+) \exp[-\tfrac{1}{2}\alpha^2(\rho^2 + \lambda^2)], \tag{17}$$

where we have explicitly shown only the highest state of an orbital angular momentum multiplet and where

$$\alpha \equiv (3Km)^{1/4} \tag{18}$$

and

$$\omega = (3K/m)^{1/2}. \tag{19}$$

By combining these spatial wave functions with quark spin, flavor, and color wave functions to obtain totally antisymmetric wave functions, one can construct the nonstrange states associated with the five $N = 2$ SU(6) supermultiplets of the harmonic-oscillator model. These states are discussed and tabulated in Appendix B and Table I where we introduce the notation $|X^{2S+1}L_\pi J^P\rangle$ in which $X = N$ or Δ, S is the quark spin, $L = S, P, D, \ldots$ is the orbital angular momentum, $\pi = S$, M, or A is the permutational symmetry (symmetric, mixed, antisymmetric) of the spatial wave function, and J^P is the total angular momentum and parity of the state. The wave function (11) is of the type S_S and leads to nonstrange states associated with the $(56', 0^+)$ SU(6) multiplet, (12) and (13) are wave functions of mixed symmetry which lead to states of the type S_M associated with the $(70, 0^+)$, (14) is D_S corresponding to $(56, 2^+)$, (15) and (16) lead to D_M associated with $(70, 2^+)$, and finally (17) is P_A and leads to states associated with the $(20, 1^+)$ SU(6) supermultiplet. The states $|X^{2S+1}L_\pi J^P\rangle$ thus correspond exactly to SU(6) states $|X^{2S+1}[\mu, L^P]J^P\rangle$, where μ is the SU(6) multiplicity, and where $\pi = S$, M and A correspond to $\mu = 56$, 70, and 20, respectively. However, this simple correspondence will be broken when we come to consider the $S = -1$ sector, and we shall find the spectroscopic notation we have adopted more convenient.

In the harmonic-oscillator model (i.e., if $U = 0$) these zeroth-order states are, as already noted, degenerate. If $U \neq 0$, these states split apart in mass; however, permutational symmetry ensures

TABLE I. The nonstrange excited baryons of positive parity.

	$^2 8$	$^4 8$	$^2 10$	$^4 10$
$J^P = \frac{1}{2}^+$	$N^2S_S\frac{1}{2}^+$	$N^4D_M\frac{1}{2}^+$	$\Delta^2S_M\frac{1}{2}^+$	$\Delta^4D_S\frac{1}{2}^+$
	$N^2S_M\frac{1}{2}^+$			
	$N^2P_A\frac{1}{2}^+$			
$J^P = \frac{3}{2}^+$	$N^2D_S\frac{3}{2}^+$	$N^4S_M\frac{3}{2}^+$	$\Delta^2D_M\frac{3}{2}^+$	$\Delta^4S_S\frac{3}{2}^+$
	$N^2D_M\frac{3}{2}^+$	$N^4D_M\frac{3}{2}^+$		$\Delta^4D_S\frac{3}{2}^+$
	$N^2P_A\frac{3}{2}^+$			
$J^P = \frac{5}{2}^+$	$N^2D_S\frac{5}{2}^+$	$N^4D_M\frac{5}{2}^+$	$\Delta^2D_M\frac{5}{2}^+$	$\Delta^4D_S\frac{5}{2}^+$
	$N^2D_M\frac{5}{2}^+$			
$J^P = \frac{7}{2}^+$		$N^4D_M\frac{7}{2}^+$		$\Delta^4D_S\frac{7}{2}^+$

that the energy of the states ψ_{00}^{ρ} and ψ_{00}^{λ} will remain the same as will the energies of the states ψ_{22}^{ρ} and ψ_{22}^{λ}. Thus in the general case although there are seven wave functions (11)–(17) there will be only five energies which we may denote by $E(S_S)=E(56',0^+)$, $E(S_M)=E(70,0^+)$, $E(D_S)=E(56,2^+)$, $E(D_M)=E(70,2^+)$, and $E(P_A)=E(20,1^+)$. Not knowing $U(r_{ij})$ it would still seem that the introduction of five unknown constants to describe the zeroth-order energies of these five supermultiplets would be inevitable. While this is true in principle, in practice these five energies are rather tightly constrained by a simple rule: In first-order perturbation theory *any potential $U(r_{ij})$ will split the $N=2$ harmonic-oscillator energies into exactly the same pattern.*[12] This pattern, shown in Fig. 1, has the property that the five degenerate multiplets are always ordered as

$$E(S_S)=E(56',0^+)=E_0-\Delta, \tag{20}$$

$$E(S_M)=E(70,0^+)=E_0-\tfrac{1}{2}\Delta, \tag{21}$$

$$E(D_S)=E(56,2^+)=E_0-\tfrac{3}{5}\Delta, \tag{22}$$

$$E(D_M)=E(70,2^+)=E_0-\tfrac{2}{5}\Delta, \tag{23}$$

$$E(P_A)=E(20,1^+)=E_0. \tag{24}$$

This rule is proved in Appendix A, which also includes a discussion of the values for E_0 and Δ appropriate to these multiplets. It is worth noting that for an attractive potential (such as the Coulomb-type potential expected from QCD), this pattern automatically makes the states associated with the $(56',0^+)$ multiplet low-lying (as indicated by the Roper resonance) and makes the unobserved

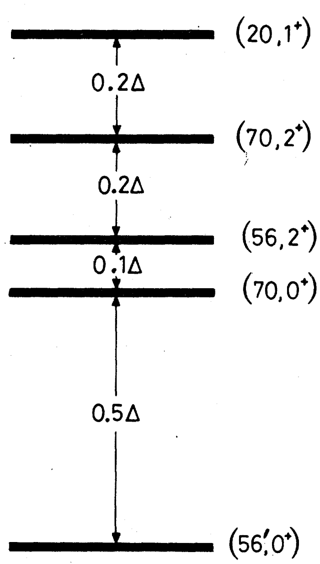

FIG. 1. The zeroth-order pattern of $N=2$ supermultiplets.

$(20,1^+)$ multiplet lie very high. Since this rule is valid only in first order, and since the perturbation involved is substantial, it is not necessarily very accurate. We have accordingly considered allowing the zeroth-order energies of the five supermultiplets to be independent parameters, but find that the empirical values we determine in this way are in excellent agreement with the spacings (20)–(24). We believe this result is a strong indication that this approach to the description of these states is sensible.

We have so far discussed only the zeroth-order energies of these states; we have not yet considered their zeroth-order wave functions. In view of the success of the first-order formulas (20)–(24), we simply assume that the harmonic-oscillator wave functions remain an adequate approximation to the true wave functions even though U is substantial. This approximation certainly worked well for the negative-parity P-wave baryons, and the effects of $U(r_{ij})$ should be quite similar there and here.

B. The $S=-1$ sector

When $m_1=m_2=m$ and $m_3=m'$, the harmonic-oscillator Hamiltonian becomes

$$H_0=\frac{p_\rho^2}{2m}+\frac{p_\rho^2}{2m_\lambda}+\frac{3}{2}K(\rho^2+\lambda^2), \tag{25}$$

where $\vec{\rho}$, $\vec{\lambda}$, and $\vec{p}_\rho$ are as previously defined and where

$$\vec{p}_\lambda=m_\lambda\frac{d\vec{\lambda}}{dt} \tag{26}$$

with

$$m_\lambda=\frac{3mm'}{2m+m'}\ . \tag{27}$$

The eigenstates of this Hamiltonian are quite distinct from those of the $S=0$ sector as the degeneracy between the ρ and λ normal modes has been broken:

$$\omega_\rho=\left(\frac{3K}{m}\right)^{1/2},\quad \omega_\lambda=\left(\frac{3K}{m_\lambda}\right)^{1/2}, \tag{28}$$

where $\omega_\lambda<\omega_\rho$ here since $x\equiv m_d/m_s\simeq 0.6$. The eigenfunctions are

$$\psi_{00}^{\lambda\lambda}=\left(\frac{2}{3}\right)^{1/2}\frac{\alpha_\rho^{3/2}\alpha_\lambda^{7/2}}{\pi^{3/2}}(\lambda^2-\tfrac{3}{2}\alpha_\lambda^{-2})\times\exp(-\tfrac{1}{2}\alpha_\rho^2\rho^2-\tfrac{1}{2}\alpha_\lambda^2\lambda^2), \tag{29}$$

$$\psi_{00}^{\rho\lambda}=\frac{2}{\sqrt{3}}\frac{\alpha_\rho^{5/2}\alpha_\lambda^{5/2}}{\pi^{3/2}}\vec{\rho}\cdot\vec{\lambda}\exp(-\tfrac{1}{2}\alpha_\rho^2\rho^2-\tfrac{1}{2}\alpha_\lambda^2\lambda^2), \tag{30}$$

$$\psi_{00}^{\rho\rho}=\left(\frac{2}{3}\right)^{1/2}\frac{\alpha_\rho^{7/2}\alpha_\lambda^{3/2}}{\pi^{3/2}}(\rho^2-\tfrac{3}{2}\alpha_\rho^{-2})\times\exp(-\tfrac{1}{2}\alpha_\rho^2\rho^2-\tfrac{1}{2}\alpha_\lambda^2\lambda^2), \quad (31)$$

$$\psi_{22}^{\lambda\lambda}=\frac{1}{\sqrt{2}}\frac{\alpha_\rho^{3/2}\alpha_\lambda^{7/2}}{\pi^{3/2}}\lambda_+\lambda_+\exp(-\tfrac{1}{2}\alpha_\rho^2\rho^2-\tfrac{1}{2}\alpha_\lambda^2\lambda^2), \quad (32)$$

$$\psi_{22}^{\rho\lambda}=\frac{\alpha_\rho^{5/2}\alpha_\lambda^{5/2}}{\pi^{3/2}}\rho_+\lambda_+\exp(-\tfrac{1}{2}\alpha_\rho^2\rho^2-\tfrac{1}{2}\alpha_\lambda^2\lambda^2), \quad (33)$$

$$\psi_{22}^{\rho\rho}=\frac{1}{\sqrt{2}}\frac{\alpha_\rho^{7/2}\alpha_\lambda^{3/2}}{\pi^{3/2}}\rho_+\rho_+\exp(-\tfrac{1}{2}\alpha_\rho^2\rho^2-\tfrac{1}{2}\alpha_\lambda^2\lambda^2), \quad (34)$$

$$\psi_{11}^{\rho\lambda}=\frac{\alpha_\rho^{5/2}\alpha_\lambda^{5/2}}{\pi^{3/2}}(\rho_+\lambda_3-\rho_3\lambda_+)\times\exp(-\tfrac{1}{2}\alpha_\rho^2\rho^2-\tfrac{1}{2}\alpha_\lambda^2\lambda^2), \quad (35)$$

where once again we have explicitly shown only the top state of an angular momentum multiplet and where

$$\alpha_\rho^2\equiv(3Km_\rho)^{1/2}=\alpha,\quad \alpha_\lambda^2=(3Km_\lambda)^{1/2}. \quad (36)$$

Thus even in the case $U=0$ the once degenerate harmonic-oscillator levels are split apart with $\psi_{00}^{\lambda\lambda}$ and $\psi_{2m}^{\lambda\lambda}$ lowest at $\frac{3}{2}\omega_\rho+\frac{7}{2}\omega_\lambda$, $\psi_{00}^{\rho\lambda}$, $\psi_{1m}^{\rho\lambda}$, and $\psi_{2m}^{\rho\lambda}$ at $\frac{5}{2}\omega_\rho+\frac{5}{2}\omega_\lambda$, and with $\psi_{00}^{\rho\rho}$ and $\psi_{2m}^{\rho\rho}$ the highest at $\frac{7}{2}\omega_\rho+\frac{3}{2}\omega_\lambda$. The case $U\neq 0$ is accordingly somewhat more complicated here than it was in the nonstrange sector. In the SU(3) limit the effects of U on the states (29) to (35) are obtained in terms of the constants E_0 and Δ of the nonstrange sector:

$$E(S_{\rho\rho})=E(S_{\lambda\lambda})=E[\psi_{00}^{\rho\rho}]=E[\psi_{00}^{\lambda\lambda}]=E_0-\tfrac{3}{4}\Delta, \quad (37)$$

$$\langle S_{\rho\rho}|U|S_{\lambda\lambda}\rangle=\langle\psi_{00}^{\rho\rho}|U|\psi_{00}^{\lambda\lambda}\rangle=-\tfrac{1}{4}\Delta, \quad (38)$$

$$E(S_{\rho\lambda})=E[\psi_{00}^{\rho\lambda}]=E_0-\tfrac{1}{2}\Delta, \quad (39)$$

$$E(D_{\rho\rho})=E(D_{\lambda\lambda})=E[\psi_{2m}^{\lambda\lambda}]=E_0-\tfrac{3}{10}\Delta, \quad (40)$$

$$\langle D_{\rho\rho}|U|D_{\lambda\lambda}\rangle=\langle\psi_{2m}^{\rho\rho}|U|\psi_{2m}^{\lambda\lambda}\rangle=-\tfrac{1}{10}\Delta, \quad (41)$$

$$E(D_{\rho\lambda})=E[\psi_{2m}^{\rho\lambda}]=E_0-\tfrac{1}{5}\Delta, \quad (42a)$$

$$E(P_{\rho\lambda})=E[\psi_{1m}^{\rho\lambda}]=E_0. \quad (42b)$$

On the other hand we have just seen that in the limit $U=0$ the effect of $m_s\neq m_d$ is to lower the energy of a λ excitation relative to a ρ excitation by

$$\Delta\omega=\omega\left[1-\left(\frac{m}{m_\lambda}\right)^{1/2}\right]. \quad (43)$$

Thus if we were to treat both $U\neq 0$ and $m_s\neq m_d$ as small perturbations, we would, after adding to all the energies a term δE_0 corresponding to the difference between the zeroth-order energies of the ground states in the $S=-1$ and $S=0$ sectors, simply subtract $2\Delta\omega$ from the energies of the states $S_{\lambda\lambda}$ and $D_{\lambda\lambda}$ and $\Delta\omega$ from the energies of $S_{\rho\lambda}$, $P_{\rho\lambda}$, and $D_{\rho\lambda}$. Since Δ is a substantial quantity, however, this approximation is probably not a very good one as it assumes that the effect of $m_s\neq m_d$ will be just as strong in the S_S states, which are only about 500 MeV above the ground state, as in the P_A states which lie roughly another 500 MeV higher. The effect of $m_s\neq m_d$ corresponds to a kinetic energy perturbation

$$\Delta K=-(1-x)p_3^2/2m, \quad (44)$$

and would presumably be quite different in the two cases. We have accordingly adopted an alternative prescription to compensate for this effect: We continue to assume that the effect of $m_s\neq m_d$ is to decrease the energy of a λ excitation by a factor $(m/m_\lambda)^{1/2}$, but we apply this factor to the U-perturbed energies of these states. Explicit calculation shows that this assumption has little effect on our predicted spectrum; it does have a noticeable effect however on our predictions of some mixing angles between low-lying strange states associated with the $(56',0^+)$ and $(70,0^+)$ SU(6) multiplets so that one should view these particular predictions with caution.

We turn now to the construction of the $S=-1$ states associated with the five $N=2$ SU(6) supermultiplets of the harmonic-oscillator model. With the strange quark singled out as quark 3, it is only the $1\longleftrightarrow 2$ symmetry of the states which remains relevant; we have accordingly introduced in Appendix B the isospin wave functions $\phi_\Sigma=(1/\sqrt{2})(ud+du)s$ and $\phi_\Lambda\equiv(1/\sqrt{2})(ud-du)s$ appropriate to the description of the Λ and Σ^0 states in this framework. Since the states of the types $\rho\rho$, $\rho\lambda$, and $\lambda\lambda$ are symmetric, antisymmetric, and symmetric respectively under the interchange $1\longleftrightarrow 2$, one can with the aid of the usual spin wave functions construct states that are flavor, space, and spin symmetric under interchange of the two nonstrange quarks. These *uds* basis states are discussed and tabulated in Appendix B and Table II where they are labelled by $|Y^{2S+1}_\sigma L_\sigma J^P\rangle$, where $Y=\Lambda$ or Σ^0; S, L, and J^P are as in the nonstrange sector; and $\sigma=\rho\rho$, $\rho\lambda$, $\lambda\lambda$. One can of course also discuss these states in terms of the SU(6) basis $|Y^{2S+1}L_\pi J^P\rangle$, and we have accordingly also discussed these states in Appendix B along with the relation between the two descriptions. These states may be found listed in Table III. While we continue to favor the *uds* basis for the light it sheds

TABLE II. The strangeness -1 excited baryons of positive parity in the *uds* basis.

	$^2\Lambda$	$^4\Lambda$	$^2\Sigma$	$^4\Sigma$
$J^P=\frac{1}{2}^+$	$\Lambda^2S_{\rho\rho}\frac{1}{2}^+$	$\Lambda^4D_{\rho\lambda}\frac{1}{2}^+$	$\Sigma^2S_{\rho\rho}\frac{1}{2}^+$	$\Sigma^4D_{\rho\rho}\frac{1}{2}^+$
	$\Lambda^2S_{\lambda\lambda}\frac{1}{2}^+$	$\Lambda^4P_{\rho\lambda}\frac{1}{2}^+$	$\Sigma^2S_{\lambda\lambda}\frac{1}{2}^+$	$\Sigma^4D_{\rho\rho}\frac{1}{2}^+$
	$\Lambda^2S_{\rho\lambda}\frac{1}{2}^+$		$\Sigma^2S_{\rho\lambda}\frac{1}{2}^+$	
	$\Lambda^2P_{\rho\lambda}\frac{1}{2}^+$		$\Sigma^2P_{\rho\lambda}\frac{1}{2}^+$	
$J^P=\frac{3}{2}^+$	$\Lambda^2D_{\rho\rho}\frac{3}{2}^+$	$\Lambda^4S_{\rho\lambda}\frac{3}{2}^+$	$\Sigma^2D_{\rho\rho}\frac{3}{2}^+$	$\Sigma^4S_{\rho\rho}\frac{3}{2}^+$
	$\Lambda^2D_{\lambda\lambda}\frac{3}{2}^+$	$\Lambda^4D_{\rho\lambda}\frac{3}{2}^+$	$\Sigma^2D_{\lambda\lambda}\frac{3}{2}^+$	$\Sigma^4S_{\lambda\lambda}\frac{3}{2}^+$
	$\Lambda^2D_{\rho\lambda}\frac{3}{2}^+$	$\Lambda^4P_{\rho\lambda}\frac{3}{2}^+$	$\Sigma^2D_{\rho\lambda}\frac{3}{2}^+$	$\Sigma^4D_{\rho\rho}\frac{3}{2}^+$
	$\Lambda^2P_{\rho\lambda}\frac{3}{2}^+$		$\Sigma^2P_{\rho\lambda}\frac{3}{2}^+$	$\Sigma^4D_{\lambda\lambda}\frac{3}{2}^+$
$J^P=\frac{5}{2}^+$	$\Lambda^2D_{\rho\rho}\frac{5}{2}^+$	$\Lambda^4D_{\rho\lambda}\frac{5}{2}^+$	$\Sigma^2D_{\rho\rho}\frac{5}{2}^+$	$\Sigma^4D_{\rho\rho}\frac{5}{2}^+$
	$\Lambda^2D_{\lambda\lambda}\frac{5}{2}^+$	$\Lambda^4P_{\rho\lambda}\frac{5}{2}^+$	$\Sigma^2D_{\lambda\lambda}\frac{5}{2}^+$	$\Sigma^4D_{\lambda\lambda}\frac{5}{2}^+$
	$\Lambda^2D_{\rho\lambda}\frac{5}{2}^+$		$\Sigma^2D_{\rho\lambda}\frac{5}{2}^+$	
$J^P=\frac{7}{2}^+$		$\Lambda^4D_{\rho\lambda}\frac{7}{2}^+$		$\Sigma^4D_{\rho\rho}\frac{7}{2}^+$
				$\Sigma^4D_{\lambda\lambda}\frac{7}{2}^+$

on the physics (see Sec. IV), we shall also quote our results in the SU(6) basis for ease of comparison with other work and with the nonstrange sector.

III. TURNING ON THE HYPERFINE INTERACTION

With the zeroth-order energies and wave functions established according to the methods outlined in the previous section and explicitly displayed in Appendices A and B, we are in a position to calculate matrix elements of the hyperfine interaction. In the nonstrange sector the procedure is completely straightforward although there is certainly a new element appearing: The hyperfine interactions will not only lead to mixing with-

TABLE III. The strangeness -1 excited baryons of positive parity in the SU(6) basis.

$J^P=\frac{1}{2}^+$	$\Lambda_1{}^2S_M\frac{1}{2}^+$	$\Lambda_1{}^4P_A\frac{1}{2}^+$	$\Lambda_8{}^2S_S\frac{1}{2}^+$	$\Lambda_8{}^4D_M\frac{1}{2}^+$	$\Sigma_{10}{}^2S_M\frac{1}{2}^+$	$\Sigma_{10}{}^4D_S\frac{1}{2}^+$
			$\Lambda_8{}^2S_M\frac{1}{2}^+$	$\Sigma_8{}^4D_M\frac{1}{2}^+$		
			$\Lambda_8{}^2P_A\frac{1}{2}^+$			
			$\Sigma_8{}^2S_S\frac{1}{2}^+$			
			$\Sigma_8{}^2S_M\frac{1}{2}^+$			
			$\Sigma_8{}^2P_A\frac{1}{2}^+$			
$J^P=\frac{3}{2}^+$	$\Lambda_1{}^2D_M\frac{3}{2}^+$	$\Lambda_1{}^4P_A\frac{3}{2}^+$	$\Lambda_8{}^2D_S\frac{3}{2}^+$	$\Lambda_8{}^4S_M\frac{3}{2}^+$	$\Sigma_{10}{}^2D_M\frac{3}{2}^+$	$\Sigma_{10}{}^4S_S\frac{3}{2}^+$
			$\Lambda_8{}^2D_M\frac{3}{2}^+$	$\Lambda_8{}^4D_M\frac{3}{2}^+$		$\Sigma_{10}{}^4D_S\frac{3}{2}^+$
			$\Lambda_8{}^2P_A\frac{3}{2}^+$	$\Sigma_8{}^4S_M\frac{3}{2}^+$		
			$\Sigma_8{}^2D_S\frac{3}{2}^+$	$\Sigma_8{}^4D_M\frac{3}{2}^+$		
			$\Sigma_8{}^2D_M\frac{3}{2}^+$			
			$\Sigma_8{}^2P_A\frac{3}{2}^+$			
$J^P=\frac{5}{2}^+$	$\Lambda_1{}^2D_M\frac{5}{2}^+$	$\Lambda_1{}^4P_A\frac{5}{2}^+$	$\Lambda_8{}^2D_S\frac{5}{2}^+$	$\Lambda_8{}^4D_M\frac{5}{2}^+$	$\Sigma_{10}{}^2D_M\frac{5}{2}^+$	$\Sigma_{10}{}^4D_S\frac{5}{2}^+$
			$\Lambda_8{}^2D_M\frac{5}{2}^+$	$\Sigma_8{}^4D_M\frac{5}{2}^+$		
			$\Sigma_8{}^2D_S\frac{5}{2}^+$			
			$\Sigma_8{}^2D_M\frac{5}{2}^+$			
$J^P=\frac{7}{2}^+$				$\Lambda_8{}^4D_M\frac{7}{2}^+$		$\Sigma_{10}{}^4D_S\frac{7}{2}^+$
				$\Sigma_8{}^4D_M\frac{7}{2}^+$		

in a given SU(6) multiplet, as in the $(70, 1^-)$ baryons, but also in general to mixing of states belonging to different SU(6) multiplets. Thus, for example, since the states $N^2D_S\frac{5}{2}^+$, $N^2D_M\frac{5}{2}^+$, and $N^4D_M\frac{5}{2}^+$ all have the same isospin and J^P, they can in general mix with each other. (In this particular case, in fact, we shall find that the first two of these tend to be strongly mixed.) The $S=-1$ sector, while still straightforward, has the additional complication of the U-induced mixings between ρ^2- and λ^2-type states. The nature of these effects is easy to understand: For a harmonic oscillator ρ^2 and λ^2 are decoupled eigenmodes, but U couples them. In the limit where the mixing by U is very strong the eigenstates of the Hamiltonian would become

$$\psi_{00}^{S\prime}=\frac{1}{\sqrt{2}}(\psi_{00}^{\rho\rho}+\psi_{00}^{\lambda\lambda}), \quad (45)$$

$$\psi_{00}^{\lambda}=\frac{1}{\sqrt{2}}(\psi_{00}^{\rho\rho}-\psi_{00}^{\lambda\lambda}), \quad (46)$$

and

$$\psi_{22}^{S}=\frac{1}{\sqrt{2}}(\psi_{22}^{\rho\rho}+\psi_{22}^{\lambda\lambda}), \quad (47)$$

$$\psi_{22}^{\lambda}=\frac{1}{\sqrt{2}}(\psi_{22}^{\rho\rho}-\psi_{22}^{\lambda\lambda}), \quad (48)$$

and the SU(6) limit would be recovered in the absence of hyperfine interactions. Of course the $\rho\lambda$-type states are unmixed by U and so the simple *uds* interpretation of these states remains unspoiled. In fact we shall see that while $S_{\rho\rho}$ and $S_{\lambda\lambda}$ are quite strongly mixed by U, the $D_{\rho\rho}$ and $D_{\lambda\lambda}$ states remain relatively pure. Thus although the situation is not as clean here as in the negative-parity baryons where ψ^{ρ} and ψ^{λ} necessarily remained pure, the *uds* basis remains not only simpler, but also more useful. In particular, as we shall discuss at greater length in Sec. IV, just as the ψ^{ρ} states of the negative-parity baryons decouple from $\bar{K}N$,[2] so here all of the states $S_{\rho\rho}$, $S_{\rho\lambda}$, $P_{\rho\lambda}$, $D_{\rho\rho}$, and $D_{\rho\lambda}$ decouple from this channel: A one-quark operator cannot emit the s quark (into the $\bar{K}$) and at the same time deexcite the ud pair in the ρ oscillator into its ground state as would be required for a transition into a ground-state nucleon. This decoupling plays an extremely important role in the interpretation of our results in Sec. IV since most of the data in the $S=-1$ sector comes from $\bar{K}N$ scattering. In summary, in the $S=-1$ sector the states are shifted and mixed not only by $H_{\rm hyp}$ but also by U, and in a given isospin and J^P sector one must simultaneously diagonalize all of these effects.

With this overview of the calculations completed, we turn to details. In the nonstrange sector the states are completely symmetric in flavor, spin, and space under interchange of any two quarks, so it follows that

$$\langle B|H_{\rm hyp}|A\rangle=3\langle B|H_{\rm hyp}^{12}|A\rangle, \quad (49)$$

where $|A\rangle$ and $|B\rangle$ are any two states. This trick considerably simplifies the calculations. There are some other general points worth noting. Since $H_{\rm contact}^{12}$ is an operator with spin zero and orbital angular momentum zero, its matrix elements vanish between states of different quark spin or different total orbital angular momenta. It is, moreover, clear that the matrix elements of $H_{\rm contact}^{12}$ are independent of the coupling of the quark spin and the orbital angular momentum to form a total angular momentum J. Thus, for example,

$$\langle N^2D_S\tfrac{5}{2}^+|H_{\rm contact}^{12}|N^2D_S\tfrac{5}{2}^+\rangle=\langle N^2D_S\tfrac{3}{2}^+|H_{\rm contact}^{12}|N^2D_S\tfrac{3}{2}^+\rangle.$$

$H_{\rm tensor}^{12}$, on the other hand, is an operator with spin 2 and orbital angular momentum 2. It cannot therefore connect two $S=\frac{1}{2}$ states, nor can it take $L=0\longleftrightarrow L=0$ or $L=0\longleftrightarrow L=1$.

The $S=-1$ states are somewhat more complicated, as usual. In the $(70, 1^-)$ states where we could find the exact eigenfunctions for $m_\lambda\neq m_\rho$, we simply proceeded by brute force, the calculations being considerably lengthier since (49) could no longer be used and since individual matrix elements were more complicated. Here, in view of the approximations we have been forced to use as a result of the inadequacy of the harmonic potential, we forego the calculation of the effects of wave-function distortion on hyperfine matrix elements (which were small anyway) and make our calculations in the limit $\alpha_\rho=\alpha_\lambda$. Of course we continue to take into account the $1/m_im_j$ dependence of the hyperfine interaction:

$$H_{\rm hyp}=\tilde{H}_{\rm hyp}^{12}+x(\tilde{H}_{\rm hyp}^{13}+\tilde{H}_{\rm hyp}^{23}), \quad (50)$$

where $\tilde{H}_{\rm hyp}^{ij}$ is (4) with $m_i=m_j=m_d$ and $x=m_d/m_s$.

The main difficulty in the calculations is simply their length as a glance at the relevant states in Appendix B will make evident; in an attempt to minimize errors each of us has calculated all matrix elements independently. The results are displayed in Appendix C in the SU(6) basis; the matrix elements in the *uds* basis may be obtained using the results of Appendix B. Given these matrix elements and the zeroth-order matrix elements of the Hamiltonian discussed in Appendix A, the calculation becomes a problem in matrix diagonalization once one knows the numerical values of the parameters appearing in the matrices. Almost all of these parameters have been previously determined; for example, all hyperfine matrix elements are expressed in terms of

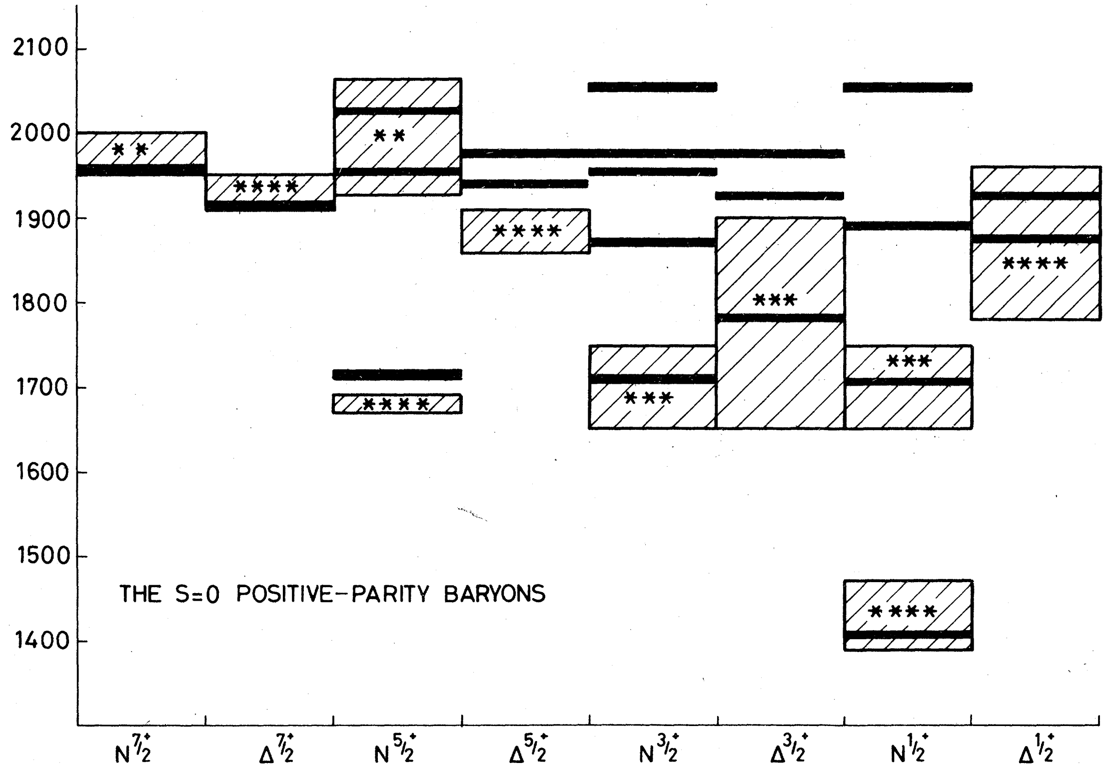

FIG. 2. Comparison of the predicted and observed spectrum of low-lying $S=0$ positive-parity excited baryons (mass in MeV). The solid bars are the predictions of the text. The shaded regions give the likely mass range for those resonances listed by the Particle Data Group (Ref. 16) as having been reported in at least two partial-wave analyses.

$$\delta \equiv \frac{4\alpha_s \alpha^3}{3\sqrt{2\pi}\, m_d^2} \simeq 300 \text{ MeV}, \tag{51}$$

from the known $\Delta - N$ mass difference in the ground states. Similarly, $x \equiv m_d/m_s$ and $\Delta m \equiv m_s - m_d$ are also known from our previous work[1,2,3] (see Appendix A). Of course the value $x \simeq 0.6$ which we use may also be obtained from the measured ratio of the magnetic moments of the proton and Λ[13]:

$$x \simeq -\frac{3\mu_\Lambda}{\mu_p} = 0.61 \pm 0.05 . \tag{52}$$

The only new parameters which we must introduce are therefore the masses E_0 and Δ of Eqs. (20)–(24) which are given and discussed in Appendix A.

The spectrum which follows from the diagonalization of the resulting matrices is displayed in Figs. 2 and 3, and both the spectrum and the composition of the eigenstates in terms of the *uds* and SU(6) bases are tabulated in Tables IV, V, and VI.

IV. COMPARISON TO EXPERIMENT AND DISCUSSION

Before making a comparison to experiment it is useful to first discuss some selection rules relevant to the interpretation of our results in the $S=-1$ states. The description of hyperons in the "*uds*" basis is, as mentioned previously, very informative with respect to their decay couplings. This is due to selection rules which were already noted for negative *P*-wave hyperons.[2] The ρ-excited hyperons (in which the orbital excitation is in the *ud* pair) are not allowed to decay into the $\bar{K}N$, $\bar{K}\Delta$, $\bar{K}^*N$, or $\bar{K}^*\Delta$ channels via a single-quark transition operator. This rule holds because a single-quark operator cannot at the same time emit the strange quark (into $\bar{K}$ or $\bar{K}^*$) and also deexcite the *ud* pair to the ground state. The same rule holds also for the positive-parity hyperons considered here. Of the three types of excitation which can occur: $\lambda\lambda$, $\lambda\rho$, and $\rho\rho$ only the $\lambda\lambda$ type couples to these four channels. While this selection rule is exact for harmonic-oscillator systems, it will remain valid as long as the orbital wave functions of the initial and final state are each well approximated by single wave functions of a harmonic oscillator or, more generally, as long as the orbital angular momentum of the *ud* pair is different in the initial and final states. For example, configuration mixing in the nucleon leads to violations of this selection rule.

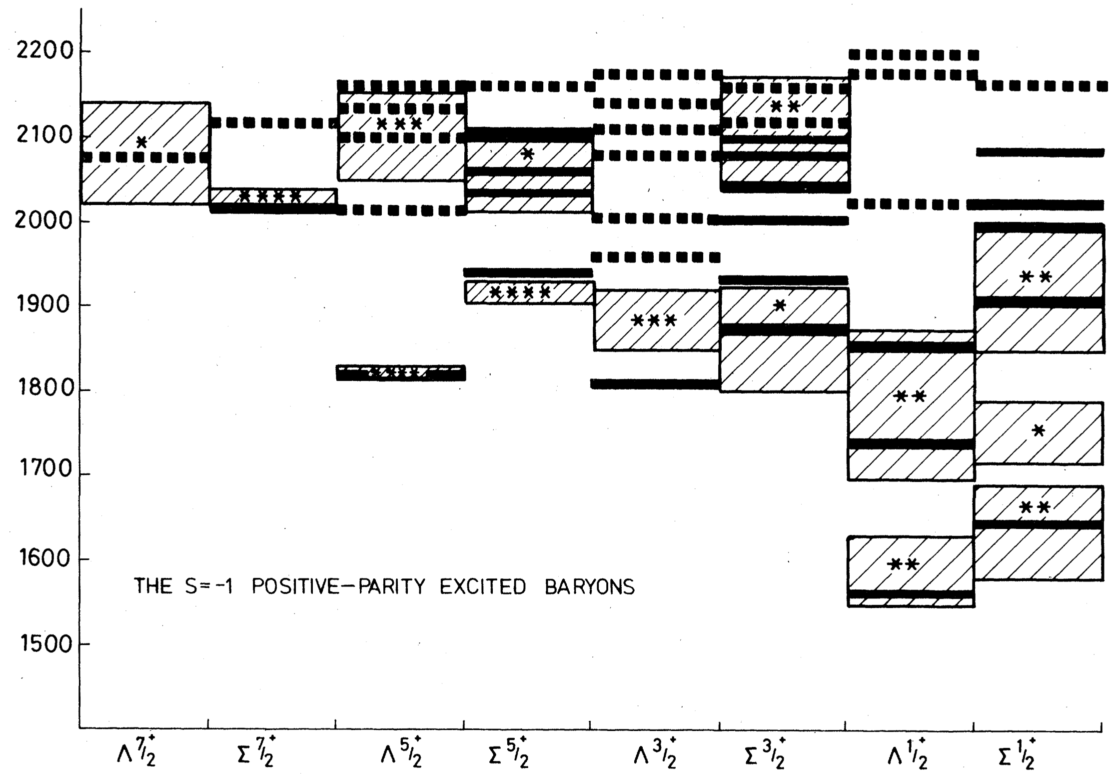

FIG. 3. Comparison of the predicted and observed spectrum of low-lying $S=-1$ positive-parity excited baryons (mass in MeV). The solid (dotted) bars are those resonances predicted by the model to be strongly (weakly) coupled to $\bar{K}N$. The shaded regions give the likely mass range for those resonances listed by the Particle Data Group (Ref. 16) as having been reported in at least two partial-wave analyses.

All these states can decay by pion emission.[14] The states $\lambda\lambda$, $\lambda\rho$, and $\rho\rho$ are all equally allowed to decay to ground-state hyperons. One could, however, distinguish two kinds of pion decay to P-wave baryons: ($\rho\rho\to\rho$, $\rho\lambda\to\rho$ or λ, and $\lambda\lambda\to\lambda$) and ($\rho\rho\to\lambda$, $\lambda\lambda\to\rho$); in a harmonic-oscillator model the amplitudes for the second kind of coupling, like $\rho\rho\to\lambda$ are suppressed by two factors of ka (where a is the size of the system) relative to couplings like $\rho\rho\to\rho$. In the bag model, where the ρ excitations correspond to excitations of nonstrange quarks and the λ excitations correspond to excitation of strange quarks these suppressed transitions are in fact forbidden as single-quark transitions as is the transition $\rho\lambda\to$ ground state. It would be interesting to know whether experimentally the "suppressed" amplitudes are in fact smaller than the "allowed" ones.

There is an extension of these selection rules to the Ξ^* sector which we do not discuss explicitly in this paper. In this channel only $\lambda\lambda$ excitations (or the λ excitations for negative-parity Ξ^*'s) are allowed to couple to the $\Xi\pi$ or $\Xi\rho$ channels, where Ξ is a ground state $\Xi(1317)$ or $\Xi(1530)$ baryon.

These selection rules are relevant to the positive-parity hyperons considered here since (as for negative-parity hyperons[2]) many of the states are almost pure in the uds basis, and one can then see at a glance whether they are allowed to couple to the $\bar{K}N$ channel. This is the generalization of "ideal mixing" for baryons from the P-wave hyperons to this case. In practice this purity is more nearly realized for D states than for S states. This is due to the relative importance of the SU(6) breaking by masses which is larger than the SU(6)-conserving "Δ splittings" in the D states but not in the S states. The borderline case is in the $\Sigma\frac{5}{2}^+$ sector where the ^4D states are pure in the uds basis, while the ^2D states are pure in the SU(6) basis. This is due to a delicate interference between hyperfine interactions and the Δ splitting.

With this background, we now turn to a detailed sector-by-sector analysis of the results:

$N\frac{7}{2}^+$: Two recent analyses[15] have reported seeing the $N(1990)\frac{7}{2}^+$,[16] and this resonance should probably now be considered as firmly established; thereby, the existence of the whole $(70, 2^+)$ multiplet which we expect in this region is also established. The reported mass values for $N(1990)\frac{7}{2}^+$ are in good agreement with its predicted posi-

TABLE IV. The calculated spectrum and composition in the $S=0$ sector.

State	Mass (MeV)	Composition					
$N\frac{7}{2}^+$	1955	1.00					$N^4D_M\frac{7}{2}^+$
$\Delta\frac{7}{2}^+$	1915	1.00					$\Delta^4D_S\frac{7}{2}^+$
$N\frac{5}{2}^+$	1715	0.88	−0.48	0.01			$N^2D_S\frac{5}{2}^+$
$N\frac{5}{2}^+$	1955	0.48	0.84	0.27			$N^2D_M\frac{5}{2}^+$
$N\frac{5}{2}^+$	2025	−0.13	−0.23	0.96			$N^4D_M\frac{5}{2}^+$
$\Delta\frac{5}{2}^+$	1940	0.94	0.38				$\Delta^4D_S\frac{5}{2}^+$
$\Delta\frac{5}{2}$	1975	−0.38	0.94				$\Delta^2D_M\frac{5}{2}^+$
$N\frac{3}{2}^+$	1710	−0.17	0.84	−0.52	0.03	0.00	$N^4S_M\frac{3}{2}^+$
$N\frac{3}{2}^+$	1870	0.75	0.34	0.28	−0.46	0.16	$N^2D_S\frac{3}{2}^+$
$N\frac{3}{2}^+$	1955	0.59	−0.05	−0.23	0.61	−0.48	$N^2D_M\frac{3}{2}^+$
$N\frac{3}{2}^+$	1980	−0.23	0.41	0.77	0.28	−0.34	$N^4D_M\frac{3}{2}^+$
$N\frac{3}{2}^+$	2060	0.11	0.08	0.12	0.58	0.79	$N^2P_A\frac{3}{2}^+$
$\Delta\frac{3}{2}^+$	1780	0.98	0.18	−0.10			$\Delta^4S_S\frac{3}{2}^+$
$\Delta\frac{3}{2}^+$	1925	−0.18	0.92	−0.36			$\Delta^4D_S\frac{3}{2}^+$
$\Delta\frac{3}{2}^+$	1975	0.03	0.36	0.94			$\Delta^2D_M\frac{3}{2}^+$
$N\frac{1}{2}^+$	1405	0.99	0.17	0.01	0.00		$N^2S_S\frac{1}{2}^+$
$N\frac{1}{2}^+$	1705	−0.15	0.94	−0.31	−0.07		$N^2S_M\frac{1}{2}^+$
$N\frac{1}{2}^+$	1890	−0.06	0.30	0.83	0.46		$N^4D_M\frac{1}{2}^+$
$N\frac{1}{2}^+$	2055	0.02	−0.08	−0.45	0.89		$N^2P_A\frac{1}{2}^+$
$\Delta\frac{1}{2}^+$	1875	0.64	0.77				$\Delta^2S_M\frac{1}{2}^+$
$\Delta\frac{1}{2}^+$	1925	0.77	−0.64				$\Delta^4D_S\frac{1}{2}^+$

tion, and it is the only state seen in this mass range in the $F17$ partial wave, as expected.

$\Delta\frac{7}{2}^+$: The well-established $\Delta(1950)\frac{7}{2}^+$[16] resonance lies very near its expected position and is, as required, the only state seen in this mass range for the $F37$ partial wave.

$\Lambda\frac{7}{2}^+$: There have been recent reports[17] of the $\Lambda(2020)\frac{7}{2}^+$[16] which, when combined with the evidence for $N(1990)\frac{7}{2}^+$, makes the existence of this resonance seem likely. The range of masses quoted for this resonance is consistent with our prediction. We also predict this resonance to decouple from the $\bar{K}N$ channel; the experimental branching ratio is in fact only 0.05 ± 0.02.

$\Sigma\frac{7}{2}^+$: We predict the existence of two $\Sigma\frac{7}{2}^+$ states, one at ~2015 MeV and one at ~2105 MeV. The lower-mass resonance can clearly be identified with the well-established $\Sigma(2030)\frac{7}{2}^+$.[16] The absence of the higher-mass resonance might be thought a problem, but in fact constitutes a success of the calculation. As is clear from Table V, which gives the composition of these two states in the *uds* basis, the upper state is pure $^4D_{\rho\rho}$ and so as discussed in Sec. III *it will be strongly decoupled from the* $\bar{K}N$ *channel*. The model therefore correctly predicts that only one resonance should be readily observed in this channel. Note that this conclusion is not obvious in the SU(6) basis of Table VI. The partial width of the observed $\Sigma(2030)$ into the $\bar{K}N$ channel is about 40 MeV which is quite consistent with our expectation of strong coupling.

$N\frac{5}{2}^+$: The position of the well-established $N(1688)\frac{5}{2}^+$[16] is rather well reproduced by the model. It is worth noting that the substantial departure of this state from its zeroth-order position arises both from diagonal contact terms and very strong mixing via the contact forces between $N^2D_S\frac{5}{2}^+$ and $N^2D_M\frac{5}{2}^+$. The $N(1688)\frac{5}{2}^+$ is therefore predicted to be a rather complete mixture of these two substates, as suggested by some recent analyses.[18] We also predict two higher states at ~1955 MeV and ~2025 MeV which correspond rather well to the $N(2000)\frac{5}{2}^+$.[16] This effect in the $F15$ partial wave has recently been seen in two new partial-wave analyses[15] and so the evidence for these states is now moderately strong.

$\Delta\frac{5}{2}^+$: There is a long-standing suggestion[19] that

TABLE V. Calculated spectrum and composition in the $S=-1$ sector in the uds basis.

State	Mass (MeV)	Composition								
$\Lambda\frac{7}{2}^+$	2070	1.00								$\Lambda^4D_{\rho\lambda}\frac{7}{2}^+$
$\Sigma\frac{7}{2}^+$	2015	0.96	0.27							$\Sigma^4D_{\lambda\lambda}\frac{7}{2}^+$
$\Sigma\frac{7}{2}^+$	2115	-0.27	0.96							$\Sigma^4D_{\rho\rho}\frac{7}{2}^+$
$\Lambda\frac{5}{2}^+$	1815	0.98	-0.10	0.16	0.00	-0.01				$\Lambda^2D_{\lambda\lambda}\frac{5}{2}^+$
$\Lambda\frac{5}{2}^+$	2010	0.14	0.93	-0.32	0.07	-0.12				$\Lambda^2D_{\rho\lambda}\frac{5}{2}^+$
$\Lambda\frac{5}{2}^+$	2095	-0.11	0.29	0.86	0.39	0.11				$\Lambda^2D_{\rho\rho}\frac{5}{2}^+$
$\Lambda\frac{5}{2}^+$	2130	0.05	-0.17	-0.36	0.87	0.28				$\Lambda^4D_{\rho\lambda}\frac{5}{2}^+$
$\Lambda\frac{5}{2}^+$	2160	0.03	0.13	-0.03	-0.29	0.95				$\Lambda^4P_{\rho\lambda}\frac{5}{2}^+$
$\Sigma\frac{5}{2}^+$	1940	0.63	0.70	-0.33	0.01	-0.02				$\Sigma^2D_{\lambda\lambda}\frac{5}{2}^+$
$\Sigma\frac{5}{2}^+$	2035	-0.16	0.13	-0.06	0.31	0.93				$\Sigma^2D_{\rho\rho}\frac{5}{2}^+$
$\Sigma\frac{5}{2}^+$	2060	0.68	-0.31	0.63	0.13	0.16				$\Sigma^2D_{\rho\lambda}\frac{5}{2}^+$
$\Sigma\frac{5}{2}^+$	2105	0.35	-0.63	-0.68	-0.09	0.13				$\Sigma^4D_{\rho\rho}\frac{5}{2}^+$
$\Sigma\frac{5}{2}^+$	2160	0.02	0.07	0.13	-0.94	0.32				$\Sigma^4D_{\lambda\lambda}\frac{5}{2}^+$
$\Lambda\frac{3}{2}^+$	1810	-0.97	-0.14	0.10	-0.02	0.10	-0.11	0.00		$\Lambda^2D_{\lambda\lambda}\frac{3}{2}^+$
$\Lambda\frac{3}{2}^+$	1960	-0.13	0.27	-0.69	0.27	-0.49	-0.33	-0.06		$\Lambda^2D_{\rho\rho}\frac{3}{2}^+$
$\Lambda\frac{3}{2}^+$	2005	0.01	0.47	-0.30	-0.28	0.72	-0.30	0.10		$\Lambda^2D_{\rho\lambda}\frac{3}{2}^+$
$\Lambda\frac{3}{2}^+$	2080	-0.05	0.20	0.09	-0.73	-0.45	-0.01	0.47		$\Lambda^4D_{\rho\lambda}\frac{3}{2}^+$
$\Lambda\frac{3}{2}^+$	2110	-0.03	-0.50	-0.63	-0.20	0.16	0.50	0.19		$\Lambda^4S_{\rho\lambda}\frac{3}{2}^+$
$\Lambda\frac{3}{2}^+$	2145	0.17	-0.58	0.02	0.06	0.07	-0.69	0.39		$\Lambda^4P_{\rho\lambda}\frac{3}{2}^+$
$\Lambda\frac{3}{2}^+$	2175	-0.05	0.26	0.08	0.53	0.08	0.26	0.76		$\Lambda^2P_{\rho\lambda}\frac{3}{2}^+$
$\Sigma\frac{3}{2}^+$	1865	0.47	0.87	0.07	0.05	0.03	0.01	-0.07	0.00	$\Sigma^4S_{\rho\rho}\frac{3}{2}^+$
$\Sigma\frac{3}{2}^+$	1935	-0.15	0.03	-0.03	0.01	0.60	0.71	-0.33	0.00	$\Sigma^4S_{\lambda\lambda}\frac{3}{2}^+$
$\Sigma\frac{3}{2}^+$	2005	-0.37	0.25	-0.13	-0.79	-0.33	0.14	-0.12	-0.10	$\Sigma^4D_{\rho\rho}\frac{3}{2}^+$
$\Sigma\frac{3}{2}^+$	2045	-0.54	0.22	0.30	0.51	-0.42	0.08	-0.35	0.04	$\Sigma^4D_{\lambda\lambda}\frac{3}{2}^+$
$\Sigma\frac{3}{2}^+$	2080	0.55	-0.34	0.08	-0.09	-0.40	0.18	-0.61	-0.05	$\Sigma^2D_{\lambda\lambda}\frac{3}{2}^+$
$\Sigma\frac{3}{2}^+$	2100	-0.11	-0.01	0.48	-0.20	0.42	-0.54	-0.40	-0.31	$\Sigma^2D_{\rho\rho}\frac{3}{2}^+$
$\Sigma\frac{3}{2}^+$	2120	-0.09	0.06	-0.58	0.04	0.38	-0.13	-0.45	0.53	$\Sigma^2D_{\rho\lambda}\frac{3}{2}^+$
$\Sigma\frac{3}{2}^+$	2165	-0.04	0.05	-0.56	0.24	-0.03	-0.07	-0.11	-0.78	$\Sigma^2P_{\rho\lambda}\frac{3}{2}^+$
$\Lambda\frac{1}{2}^+$	1555	0.75	0.66	0.09	0.01	0.00	0.00			$\Lambda^2S_{\lambda\lambda}\frac{1}{2}^+$
$\Lambda\frac{1}{2}^+$	1740	-0.56	0.69	-0.46	0.00	0.00	0.00			$\Lambda^2S_{\rho\rho}\frac{1}{2}^+$
$\Lambda\frac{1}{2}^+$	1860	-0.34	0.28	0.85	-0.29	-0.01	-0.06			$\Lambda^2S_{\rho\lambda}\frac{1}{2}^+$
$\Lambda\frac{1}{2}^+$	2020	0.12	-0.08	-0.25	-0.85	-0.10	-0.44			$\Lambda^4D_{\rho\lambda}\frac{1}{2}^+$
$\Lambda\frac{1}{2}^+$	2175	-0.03	0.02	0.06	0.45	-0.23	-0.86			$\Lambda^4P_{\rho\lambda}\frac{1}{2}^+$
$\Lambda\frac{1}{2}^+$	2205	0.00	0.00	0.00	-0.02	-0.97	0.25			$\Lambda^2P_{\rho\lambda}\frac{1}{2}^+$
$\Sigma\frac{1}{2}^+$	1640	0.84	0.53	0.11	0.01	0.00	0.00			$\Sigma^2S_{\lambda\lambda}\frac{1}{2}^+$
$\Sigma\frac{1}{2}^+$	1910	-0.23	0.51	-0.76	0.14	-0.29	0.05			$\Sigma^2S_{\rho\rho}\frac{1}{2}^+$
$\Sigma\frac{1}{2}^+$	1995	-0.19	0.31	-0.02	0.28	0.88	-0.12			$\Sigma^2S_{\rho\lambda}\frac{1}{2}^+$
$\Sigma\frac{1}{2}^+$	2025	-0.41	0.51	0.63	0.24	-0.31	0.14			$\Sigma^4D_{\rho\rho}\frac{1}{2}^+$
$\Sigma\frac{1}{2}^+$	2080	0.19	-0.31	-0.06	0.83	-0.05	0.42			$\Sigma^4D_{\lambda\lambda}\frac{1}{2}^+$
$\Sigma\frac{1}{2}^+$	2165	0.04	-0.08	0.03	0.40	-0.21	-0.89			$\Sigma^2P_{\rho\lambda}\frac{1}{2}^+$

TABLE VI. The calculated spectrum and composition in the $S=-1$ sector in the SU(6) basis.

State	Mass (MeV)	Composition								
$\Lambda\frac{7}{2}^+$	2070	1.00								$\Lambda_8\,{}^4D_M\,\frac{7}{2}^+$
$\Sigma\frac{7}{2}^+$	2015	0.87	−0.49							$\Sigma_{10}\,{}^4D_S\,\frac{7}{2}^+$
$\Sigma\frac{7}{2}$	2115	0.49	0.87							$\Sigma_{10}\,{}^4D_M\,\frac{7}{2}^+$
$\Lambda\frac{5}{2}^+$	1815	0.81	−0.48	0.34	0.00	−0.01				$\Lambda_8\,{}^2D_S\,\frac{5}{2}^+$
$\Lambda\frac{5}{2}^+$	2010	0.12	−0.43	−0.88	−0.07	0.12				$\Lambda_1\,{}^2D_M\,\frac{5}{2}^+$
$\Lambda\frac{5}{2}^+$	2095	−0.53	−0.69	0.28	−0.39	−0.11				$\Lambda_8\,{}^2D_M\,\frac{5}{2}^+$
$\Lambda\frac{5}{2}^+$	2130	−0.22	−0.32	0.09	0.87	0.28				$\Lambda_8\,{}^4D_M\,\frac{5}{2}^+$
$\Lambda\frac{5}{2}^+$	2160	0.00	0.06	0.12	−0.29	0.95				$\Lambda_1\,{}^4P_A\,\frac{5}{2}^+$
$\Sigma\frac{5}{2}^+$	1940	0.94	0.00	−0.27	0.02	−0.20				$\Sigma_8\,{}^2D_S\,\frac{5}{2}^+$
$\Sigma\frac{5}{2}^+$	2035	−0.02	0.87	−0.19	−0.44	0.10				$\Sigma_{10}\,{}^4D_S\,\frac{5}{2}^+$
$\Sigma\frac{5}{2}^+$	2060	0.26	0.21	0.94	−0.02	−0.05				$\Sigma_8\,{}^2D_M\,\frac{5}{2}^+$
$\Sigma\frac{5}{2}^+$	2105	0.20	−0.02	0.01	0.16	0.97				$\Sigma_8\,{}^4D_M\,\frac{5}{2}^+$
$\Sigma\frac{5}{2}^+$	2160	0.06	−0.44	0.06	−0.89	0.12				$\Sigma_{10}\,{}^2D_M\,\frac{5}{2}^+$
$\Lambda\frac{3}{2}^+$	1810	0.10	−0.79	−0.35	0.49	−0.01	−0.11	0.00		$\Lambda_8\,{}^4S_M\,\frac{3}{2}^+$
$\Lambda\frac{3}{2}^+$	1960	−0.49	0.10	−0.69	−0.29	0.27	−0.33	−0.05		$\Lambda_8\,{}^2D_S\,\frac{3}{2}^+$
$\Lambda\frac{3}{2}^+$	2005	0.72	0.34	−0.44	0.01	−0.28	−0.30	0.10		$\Lambda_1\,{}^2D_M\,\frac{3}{2}^+$
$\Lambda\frac{3}{2}^+$	2080	−0.45	0.11	−0.06	0.19	−0.73	−0.01	0.47		$\Lambda_8\,{}^2D_M\,\frac{3}{2}^+$
$\Lambda\frac{3}{2}^+$	2110	0.16	−0.37	−0.21	−0.68	−0.20	0.50	0.19		$\Lambda_8\,{}^4D_M\,\frac{3}{2}^+$
$\Lambda\frac{3}{2}^+$	2145	0.06	−0.29	0.39	−0.36	0.05	−0.69	0.39		$\Lambda_1\,{}^4P_A\,\frac{3}{2}^+$
$\Lambda\frac{3}{2}^+$	2175	0.07	0.14	−0.10	0.21	0.53	0.26	0.76		$\Lambda_8\,{}^2P_A\,\frac{3}{2}^+$
$\Sigma\frac{3}{2}^+$	1865	0.95	−0.29	0.02	0.09	−0.04	0.02	−0.06	0.00	$\Sigma_{10}\,{}^4S_S\,\frac{3}{2}^+$
$\Sigma\frac{3}{2}^+$	1935	−0.08	−0.13	0.93	−0.02	−0.29	−0.03	−0.18	0.00	$\Sigma_8\,{}^4S_M\,\frac{3}{2}^+$
$\Sigma\frac{3}{2}^+$	2005	−0.08	−0.44	−0.14	−0.66	−0.32	0.47	0.15	−0.10	$\Sigma_8\,{}^2D_S\,\frac{3}{2}^+$
$\Sigma\frac{3}{2}^+$	2045	−0.22	−0.54	−0.24	0.56	−0.50	−0.15	0.01	0.04	$\Sigma_{10}\,{}^4D_S\,\frac{3}{2}^+$
$\Sigma\frac{3}{2}^+$	2080	0.15	0.63	−0.15	0.00	−0.72	0.12	−0.14	−0.05	$\Sigma_8\,{}^2D_M\,\frac{3}{2}^+$
$\Sigma\frac{3}{2}^+$	2100	−0.08	−0.06	−0.08	0.20	0.19	0.48	−0.76	−0.31	$\Sigma_8\,{}^4D_M\,\frac{3}{2}^+$
$\Sigma\frac{3}{2}^+$	2120	−0.02	−0.11	−0.17	−0.38	−0.06	−0.44	−0.57	0.53	$\Sigma_{10}\,{}^2D_M\,\frac{3}{2}^+$
$\Sigma\frac{3}{2}^+$	2165	0.00	−0.07	−0.07	−0.22	−0.06	−0.57	−0.10	−0.78	$\Sigma_8\,{}^2P_A\,\frac{3}{2}^+$
$\Lambda\frac{1}{2}^+$	1555	0.99	0.02	0.10	0.02	0.00	0.00			$\Lambda_8\,{}^2S_S\,\frac{1}{2}^+$
$\Lambda\frac{1}{2}^+$	1740	0.09	0.30	−0.95	−0.01	0.00	0.00			$\Lambda_8\,{}^2S_M\,\frac{1}{2}^+$
$\Lambda\frac{1}{2}^+$	1860	−0.04	0.91	0.29	−0.29	−0.01	−0.06			$\Lambda_1\,{}^2S_M\,\frac{1}{2}^+$
$\Lambda\frac{1}{2}^+$	2020	0.03	−0.28	−0.08	−0.85	−0.09	−0.44			$\Lambda_8\,{}^4D_M\,\frac{1}{2}^+$
$\Lambda\frac{1}{2}^+$	2175	−0.01	0.07	0.02	0.45	−0.23	−0.86			$\Lambda_1\,{}^4P_A\,\frac{1}{2}^+$
$\Lambda\frac{1}{2}^+$	2205	0.00	0.00	0.00	−0.01	−0.97	0.25			$\Lambda_8\,{}^2P_A\,\frac{1}{2}^+$
$\Sigma\frac{1}{2}^+$	1640	0.97	0.23	−0.08	0.00	0.01	0.00			$\Sigma_8\,{}^2S_S\,\frac{1}{2}^+$
$\Sigma\frac{1}{2}^+$	1910	0.20	−0.91	−0.17	−0.10	0.30	0.05			$\Sigma_8\,{}^2S_M\,\frac{1}{2}^+$
$\Sigma\frac{1}{2}^+$	1995	0.08	−0.27	0.23	0.82	−0.42	−0.12			$\Sigma_{10}\,{}^2S_M\,\frac{1}{2}^+$
$\Sigma\frac{1}{2}^+$	2025	0.07	−0.01	0.91	−0.04	0.39	0.14			$\Sigma_{10}\,{}^4D_S\,\frac{1}{2}^+$
$\Sigma\frac{1}{2}^+$	2080	−0.08	0.21	−0.29	0.54	0.63	0.42			$\Sigma_8\,{}^4D_M\,\frac{1}{2}^+$
$\Sigma\frac{1}{2}^+$	2165	−0.02	0.08	−0.04	0.13	0.43	−0.89			$\Sigma_8\,{}^2P_A\,\frac{1}{2}^+$

the $\Delta(1890)\frac{5}{2}^+$ is a mixture of $\Delta^4D_S\frac{5}{2}^+$ and $\Delta^2D_M\frac{5}{2}^+$ in order to account for its strong F-wave decay to $\Delta\pi$. We indeed find a state at 1940 MeV which, while still dominantly $\Delta^4D_S\frac{5}{2}^+$, has undergone substantial mixing via the tensor force with $\Delta^2D_S\frac{5}{2}^+$ corresponding to a mixing angle of $\sim +25°$, in good agreement with the phenomenological analysis.[20] While we predict that the orthogonal partner to $\Delta(1890)\frac{5}{2}^+$ should be nearby, there is no problem associated with its not having been seen since, as pointed out in Ref. 19, for a mixing angle of $\sim +25°$ it will practically decouple from the πN channel. We consider the resolution of this problem to be further strong evidence in favor of the interaction (4).

$\Lambda\frac{5}{2}^+$: There are five resonances expected in this channel. The lowest one is clearly identified with the $\Lambda(1815)\frac{5}{2}^+$,[16] which we predict to be a state that is quite pure $^2D_{\lambda\lambda}$ and so strongly coupled to $\bar{K}N$; the observed partial width of this resonance into $\bar{K}N$ is about 50 MeV. The remaining states in this partial wave are all predicted to lie in the range from 2000–2160 MeV corresponding to the $\Lambda(2110)\frac{5}{2}^+$.[16] Note from Table IV that all these states are dominated by configurations in which there is ρ excitation so that they are predicted to be weakly coupled to $\bar{K}N$ as observed: the $\bar{K}N$ partial width of the $\Lambda(2110)\frac{5}{2}^+$ is measured to be ~ 15 MeV.[21] For comparison recall that the partial width of the pure ρ excitation $\Lambda(1830)\frac{5}{2}^-$ is 4 MeV.[21] Once again we note that while this observation is trivially made in the *uds* basis, it is completely obscured in the SU(6) basis (see Table VI).

$\Sigma\frac{5}{2}^+$: There are once again five resonances expected, and the lowest one may be rather clearly identified with the $\Sigma(1915)\frac{5}{2}^+$.[16] Once again we expect the remaining states in this partial wave to cluster together around 2100 MeV, possibly corresponding to the state $\Sigma(2070)\frac{5}{2}^+$.[16] Since, however, these states have correlations between their spin and spatial wave functions opposite to the Λ's, they are mixed very differently and there is no reason why they should not couple to $\bar{K}N$. Note that while the ^4D states are relatively pure in the *uds* basis the ^2D states are pure in the SU(6) basis; this is a result of interference between hyperfine and "Δ" interactions of opposite sign in the two different spin states.

$N\frac{3}{2}^+$: We predict that the lowest-mass state in this channel will once again be a $(56, 2^+)$ with a substantial $(70, 2^+)$ component, and this state may be identified with the $N(1810)\frac{3}{2}^+$[16] which is now reported to lie in the range from 1650 to 1750 MeV.

$\Delta\frac{3}{2}^+$: There is now a well-established resonance[16] in the region from 1650 to 1900 MeV which is consistent with the predicted resonance at 1780 MeV; the large spread of the limits on the mass of this resonance has been attributed[16] to the possible presence of additional resonances in this region in accord with our expectations.

$\Lambda\frac{3}{2}^+$: This sector is quite similar to the $\Lambda\frac{5}{2}^+$ sector, with a well established low-lying resonance, the $\Lambda(1860)\frac{3}{2}^+$,[16] which we identify as being a state that is almost pure $^2D_{\lambda\lambda}$ and therefore strongly coupled to $\bar{K}N$; the observed partial width to the $\bar{K}N$ channel for this resonance is about 40 MeV.[16] While *six* other states are expected in this partial wave, including some at relatively low masses, we consider it to be a substantial success of the model that *it predicts all of them to decouple from the* $\bar{K}N$ *channel*. We stress once again that this conclusion, while obvious in the *uds* basis of Table V, would be very difficult to see in the SU(6) basis of Table VI.

$\Sigma\frac{3}{2}^+$: Once again this sector is predicted to be very different from the corresponding $\Lambda\frac{3}{2}^+$ sector. There are a plethora of states predicted in this channel of which two should be low-lying at around 1900 MeV, while the rest cluster at around 2100 MeV. This corresponds roughly to the observed situation in that two structures are seen, one in the region around 1850 MeV[16] and the other, more well-established, around 2100 MeV.[16] Unlike the $\Lambda\frac{3}{2}^+$ sector, most of these states do couple to $\bar{K}N$. Note that the two lowest states are predicted to be fairly pure in the SU(6) basis.

$N\frac{1}{2}^+$: The model successfully accounts for both the $N(1470)\frac{1}{2}^+$[16] and $N(1780)\frac{1}{2}^+$[16] which are predicted to be dominantly $^2S_S\frac{1}{2}^+$ and $^2S_M\frac{1}{2}^+$, respectively, in accord with experiment.[22] Caution should be exercised in reading the purity of $N(1780)\frac{1}{2}^+$ from Table IV, however, as in the case of this resonance there is an important effect which we have neglected: This state mixes quite strongly with the $N(940)\frac{1}{2}^+$. (It is in fact this mixing that is responsible for the charge radius of the neutron.[9]) In general, we have found that such interband mixings are not very important, but in this case there is an especially large mixing matrix element which induces an admixture into $N(1780)\frac{1}{2}^+$ of the ground-state $^2S_S\frac{1}{2}^+$ configuration with an amplitude of $\sim\frac{1}{4}$ which is even larger than the mixing to the Roper resonance. It has in fact recently been suggested that $N(1780)\frac{1}{2}^+$ has substantial configuration mixing.[18]

$\Delta\frac{1}{2}^+$: We find that both of the states we expect in this partial wave lie within the region quoted for the well-established $\Delta(1910)\frac{1}{2}^+$.[16] We predict that these two states have been almost completely mixed by the tensor force; the rather broad range of quoted values for this resonance may be a reflection of the presence of these two states which should have quite distinct properties. This mixing could help in resolving well known difficulties in the photoproduction of these states.[23] Recently there has been a report[16] of a one-star resonance at 1550 MeV in this channel which cannot be accommodated in the model discussed here.

$\Lambda\frac{1}{2}^+$: Here we expect six states distributed in mass all the way from 1565 to 2210 MeV. The lowest state, which turns out to be an almost pure $\Lambda_8{}^2S_S\frac{1}{2}^+$ state (the octet partner to the Roper resonance), may readily be associated with the $\Lambda(1600)\frac{1}{2}^+$. Since this state has been seen in two recent partial-wave analyses,[21] it is now reasonably well established. The calculation further predicts that of the states we expect in this channel, only the low-lying ones are coupled to $\bar{K}N$ (see Table V once again); this corresponds very well with the experimental situation. Thus besides the $\Lambda(1600)\frac{1}{2}^+$ we expect only two other resonances to be observed in this channel, one at 1725 and the other at 1870 MeV. These two states lie within the region quoted for $\Lambda(1800)\frac{1}{2}^+$;[16] we anticipate that this effect will eventually be resolved into two states. As expected the observed resonances in this channel have fairly large partial widths to $\bar{K}N$.

$\Sigma\frac{1}{2}^+$: We expect a low-lying state at 1640 MeV which may rather clearly be associated with the $\Sigma(1660)\frac{1}{2}^+$.[16] While dominantly a $\Sigma_8{}^2S_S\frac{1}{2}^+$ state, this state like the Roper resonance but unlike the $\Lambda(1600)\frac{1}{2}^+$, has a significant admixture of $\Sigma_8{}^2S_M\frac{1}{2}^+$. Aside from the state at 2165 MeV which we predict to decouple from $\bar{K}N$, all the remaining states in this sector are expected to lie rather close together from 1905 to 2045 MeV, and we may associate these states with the $\Sigma(1880)\frac{1}{2}^+$[16] which is seen as an effect in this channel from 1780 to 1980 MeV. We have no place for the one-star resonance $\Sigma(1770)\frac{1}{2}^+$,[16] on the other hand, and assume that this effect will prove to be spurious.

This completes the detailed comparison of our predictions with experiment.[24] It is clear that the model successfully predicts with reasonable accuracy the position of the lowest one or two resonances in every partial wave. Moreover, in many cases, especially in the Λ sector, the model also explains plausibly why missing states are not seen in partial-wave analyses of $\bar{K}N$ scattering.

In view of the detailed agreement of these calculations with experiment, and the previously demonstrated relevance of these ideas to the ground-state baryons and the excited baryons of negative parity, it seems reasonable to us to conclude that the simple model of nonrelativistic quarks moving in a flavor-independent confining potential perturbed by the hyperfine interaction leads to an understanding of the properties of all the low-lying baryon states.

This is not to say, of course, that there are no other effects that play some role in determining the character of these states. For example, there will certainly be mass shifts and mixings due to interactions of these resonances with their decay channels,[25] and there may well be residual spin-orbit effects (see below). We would claim only that the effects discussed here are responsible for determining the principal features of these states.

The interpretation of these results at a fundamental level, however, remains open. While our initial assumptions have not been rigorously derived from QCD, the existence of strong interactions analogous in form to electromagnetic forces is certainly suggestive of QCD. The major stumbling block to the association of these forces with QCD is the apparent absence of the spin-orbit forces that would also be expected from one gluon exchange. In the negative-parity baryons we concluded that spin-orbit forces, if present at all, were reduced to a level of less than about 10% of naive expectations from one gluon exchange.[3] The situation here is very similar and once again a full-strength spin-orbit coupling is out of the question, although in this case the relative imprecision of the data and the complexity of possible mixings only allow the conclusion that any residual spin-orbit coupling is at a level of less than about 20% of the one-gluon-exchange contribution. Of the two mechanisms we have previously discussed[3] as being possible causes of the relative suppression of spin-orbit forces, the idea of a large anomalous color magnetic moment can most easily accommodate this new piece of evidence. On the other hand we believe the notion that the one-gluon exchange contribution to the spin-orbit force is being nearly cancelled by a spin-orbit interaction due to Thomas precession in the confinement potential is a more attractive one,[8] and it would clearly be interesting to know if it is also compatible with the data. Unfortunately, the considerations presented here have confirmed the warnings issued in Ref. 3 concerning the model dependence of such a cancellation by making it clear that the confining force is not harmonic, so that the calculation of the spin-orbit effects due to Thomas precession in the confinement potential becomes doubly uncertain: Not only can we not calculate the three-body contributions, but even the two-body contributions are largely uncertain. Without further understanding of the confinement forces, it is therefore very difficult to know whether this mechanism is still viable, although it is at least surprising that the cancellation should remain so effective in passing from $L^P=1^-$ to $L^P=2^+$.

These last considerations underscore the importance of trying to deduce the form of V_{conf}. The rough success of simple harmonic forces when perturbed by an attractive potential, discussed in Sec. II, make the prospects for such a study reasonably bright. Once in possession of a potential that reproduced the now known zeroth-order positions of the six lowest-lying SU(6) supermultiplets, $(56,0^+)$, $(70,1^-)$, $(56',0^+)$, $(70,0^+)$, $(56,2^+)$, and $(70,2^+)$, it will not only be possible to test the just-mentioned mechanism for spin-orbit suppression, but also to test the accuracy of the approximations we have been forced to use for the zeroth-order wave functions, and for the zeroth-order energies in the $S=-1$ sector. We hope to report on these issues shortly.

V. CONCLUSIONS

We have extended our previous study of quark hyperfine interactions in baryons, which was fairly successful in describing the properties of the negative-parity P-wave states, to low-lying positive-parity excitations. The conclusions we reach concerning these multiplets are determined by previous work apart from uncertainties concerning zero-order energies and wave functions which are taken to be approximately those of the harmonic-oscillator model.

The positive-parity baryons have been considered in the quark model by Dalitz, Horgan, and their collaborators.[26] The present work is a natural continuation of these analyses which incorporates recent prejudices about quark interactions. The model discussed here differs from earlier models in several respects. Firstly, the SU(3) breaking occurs only via quark masses. Secondly, the hyperfine interaction (contact + tensor forces) is the only spin-dependent force: Spin-orbit forces are neglected. Aside from these there are only central "nonexchange" forces between quarks; it is because of this feature that we can use nonsymmetrized *uds* wave functions. In practical terms these restrictions imply that we have a much smaller number of free parameters at our disposal as compared to earlier quark models.

The results of our calculation are very encouraging: The simple picture of flavor-independent confinement forces in which mass splittings and mixings of baryons are dominated by strong forces of magnetic-dipole–magnetic-dipole character continues to work well. While the members of these multiplets are not as well known experimentally as those of the ground state and the "70 plet," the lowest one or two resonances in almost every IJ^P channel in the $S=0$ and -1 sectors are known and are seen at the masses we expect. In addition, there is good evidence, especially from the coupling of the Λ states to $\bar{K}N$, that the mixing of these states is correctly given by the model.

It therefore seems entirely possible that the model discussed here is capable of explaining the masses and mixing properties of all low-lying baryons. While the implications of this conclusion are not completely clear at the moment, it is difficult not to associate the success of these calculations with QCD, which inspired them. In any event, if our conclusions are correct, they certainly should provide clues in the search for an understanding of the strong interactions.

Note added in proof. The effect of configuration mixing in the nucleon on some selection rules, mentioned at the beginning of Sec. IV, has now been discussed in more detail by N. Isgur, G. Karl, and R. Koniuk, Phys. Rev. Lett. 41, 1269 (1978).

ACKNOWLEDGMENTS

The authors thank respectively the Department of Theoretical Physics, Oxford University and the Theory Division, Rutherford Laboratory for their hospitality. The help of R. G. Roberts with computing, of R. L. Kelly and P. J. Litchfield with the literature and discussions with R. H. Dalitz and L. J. Reinders are also gratefully acknowledged.

This work was supported in part by the National Research Council of Canada and the Connaught Fund of the University of Toronto.

APPENDIX A: THE ZEROTH-ORDER ENERGIES OF THE POSITIVE-PARITY EXCITED BARYON SUPERMULTIPLETS

We begin this Appendix by proving that any potential

$$U=\sum_{i<j} U(r_{ij})$$

splits the $N=2$ harmonic-oscillator levels into the same pattern. We know by symmetry, first of all, that U will leave the pairs of wave functions of mixed symmetry (ψ^{ρ}_{00} and ψ^{λ}_{00}; ψ^{ρ}_{2m} and ψ^{λ}_{2m}) degenerate. Using (11) to (17) and (49) it then follows that

$$\Delta E(56',0^+)=\Delta E(S_S)=\tfrac{5}{4}a-b+\tfrac{1}{3}c, \tag{A1}$$

$$\Delta E(70,0^+)=\Delta E(S_M)=\tfrac{5}{8}a-\tfrac{1}{6}b+\tfrac{1}{6}c, \tag{A2}$$

$$\Delta E(56,2^+)=\Delta E(D_S)=\tfrac{1}{2}a+\tfrac{2}{15}c, \tag{A3}$$

$$\Delta E(70,2^+)=\Delta E(D_M)=\tfrac{1}{4}a+\tfrac{1}{3}b+\tfrac{1}{15}c, \tag{A4}$$

$$\Delta E(20,1^+)=\Delta E(P_A)=\tfrac{2}{3}b, \tag{A5}$$

where

$$a\equiv\frac{3\alpha^3}{\pi^{3/2}}\int d^3\rho\, U(\sqrt{2}\rho)e^{-\alpha^2\rho^2}\ , \tag{A6}$$

$$b\equiv\frac{3\alpha^5}{\pi^{3/2}}\int d^3\rho\, U(\sqrt{2}\rho)\rho^2 e^{-\alpha^2\rho^2}, \tag{A7}$$

$$c\equiv\frac{3\alpha^7}{\pi^{3/2}}\int d^3\rho\, U(\sqrt{2}\rho)\rho^4 e^{-\alpha^2\rho^2}\ . \tag{A8}$$

If we now define

$$E_0 \equiv 5\hbar\omega + \tfrac{2}{3}b, \tag{A9}$$

$$\Delta \equiv -\tfrac{5}{4}a + \tfrac{5}{3}b - \tfrac{1}{3}c, \tag{A10}$$

then the results (20)–(24) follow immediately.

It remains to find the best values for these two parameters empirically. A rough qualitative judgement indicates that $E_0 \simeq 2020$ MeV and $\Delta \simeq 420$ MeV; these values give for the zeroth-order energies of the five supermultiplets which are immediately relevant to the $S=0$ sector:

$$E(56', 0^+) = E(S_S) \simeq 1600 \text{ MeV}, \tag{A11}$$

$$E(70, 0^+) = E(S_M) \simeq 1810 \text{ MeV}, \tag{A12}$$

$$E(56, 2^+) = E(D_s) \simeq 1850 \text{ MeV}, \tag{A13}$$

$$E(70, 2^+) = E(D_M) \simeq 1935 \text{ MeV}, \tag{A14}$$

$$E(20, 1^+) = E(P_A) \simeq 2020 \text{ MeV}. \tag{A15}$$

Next, using the procedure outlined in Sec. II B we can calculate the zeroth-order matrix elements of the Hamiltonian in the $S=-1$ sector. One obtains in terms of the uds states

$$E(S_{\lambda\lambda}) = 1805 \text{ MeV}, \tag{A16}$$

$$E(S_{\rho\lambda}) = 1945 \text{ MeV}, \tag{A17}$$

$$E(S_{\rho\rho}) = 1895 \text{ MeV}, \tag{A18}$$

$$\langle S_{\rho\rho}|U|S_{\lambda\lambda}\rangle = -105 \text{ MeV}, \tag{A19}$$

$$E(D_{\lambda\lambda}) = 1975 \text{ MeV}, \tag{A20}$$

$$E(D_{\rho\lambda}) = 2065 \text{ MeV}, \tag{A21}$$

$$E(D_{\rho\rho}) = 2085 \text{ MeV}, \tag{A22}$$

$$\langle D_{\rho\rho}|U|D_{\lambda\lambda}\rangle = -40 \text{ MeV}, \tag{A23}$$

$$E(P_{\rho\lambda}) = 2145 \text{ MeV}, \tag{A24}$$

where, based on our previous analyses, we have taken the zeroth-order energy difference between the $S=-1$ and $S=0$ ground states to be 190 MeV. Equivalently, we have in terms of the wave functions appropriate to the SU(6) basis that in the $S=-1$ sector

$$E(S_S)_{S=-1} = 1745 \text{ MeV}, \tag{A25}$$

$$E(S_M)_{S=-1} = 1955 \text{ MeV}, \tag{A26}$$

$$\langle S_{M^\lambda}|H|S_S\rangle_{S=-1} = +45 \text{ MeV}, \tag{A27}$$

$$E(D_S)_{S=-1} = 1990 \text{ MeV}, \tag{A28}$$

$$E(D_M)_{S=-1} = 2070 \text{ MeV}, \tag{A29}$$

$$\langle D_{M^\lambda}|H|D_S\rangle_{S=-1} = +55 \text{ MeV}, \tag{A30}$$

$$E(P_A)_{S=-1} = 2145 \text{ MeV}. \tag{A31}$$

Although they are not really essential for the purposes of these calculations, there are some noteworthy aspects to these deviations from the harmonic-oscillator picture. For a short-range attractive potential the energy of $(56, 0^+)$ will be decreased more or less in parallel to $(56', 0^+)$, while $(70, 1^-)$ will move down more slowly. This allows $(56', 0^+)$ to meet $(70, 1^-)$ as required. This also means that the $(70, 1^-)-(56, 0^+)$ splitting of ~ 500 MeV is anomalously large, and that a more typical spacing is $(56, 2^+)-(70, 1^-)$ which is only half as large. In terms of the present framework, we may say that the unperturbed harmonic oscillator would have had a spacing of the order of 250 MeV. This idea is then consistent with two important facts. First, the $(56, 4^+)-(56, 2^+)$ splitting, as presumably measured by the $\Delta(2420)\frac{11}{2}^+ - \Delta(1950)\frac{7}{2}^+$ mass difference, corresponds to an oscillator spacing of ~ 250 MeV. Second, the value $\omega \sim 250$ MeV corresponds (with $m_d \simeq 350$ MeV) to a more realistic value of the proton charge radius $(\langle r^2\rangle_p{}^{1/2} \simeq 0.7$ fm) than does $\omega \sim 500$ MeV and is therefore much more amenable to treatment as a nonrelativistic system.

APPENDIX B: THE APPROXIMATE ZEROTH-ORDER STATES OF THE POSITIVE-PARITY EXCITED BARYONS

In this appendix we show the SU(6) and uds wave functions of the positive-parity baryons constructed out of the harmonic spatial functions (11) to (17) and (29) to (35), the flavor wave functions

(octet (ρ type)):

$$\phi_p^\rho = \frac{1}{\sqrt{2}}(udu - duu), \tag{B1}$$

$$\phi_n^\rho = \frac{1}{\sqrt{2}}(udd - dud), \tag{B2}$$

$$\phi_\Lambda^\rho = -\frac{1}{\sqrt{12}}(2uds - 2dus + usd - dsu - sud + sdu), \tag{B3}$$

$$\phi_{\Sigma^0}^\rho = \tfrac{1}{2}(usd - sud + dsu - sdu); \tag{B4}$$

(octet (λ type)):

$$\phi_p^\lambda = -\frac{1}{\sqrt{6}}(udu + duu - 2uud), \tag{B5}$$

$$\phi_n^\lambda = \frac{1}{\sqrt{6}}(udd + dud - 2ddu), \tag{B6}$$

$$\phi_\Lambda^\lambda = -\tfrac{1}{2}(usd - dsu + sud - sdu), \tag{B7}$$

$$\phi_{\Sigma^0}^\lambda = -\frac{1}{\sqrt{12}}(usd + sud + dsu + sdu - 2uds - 2dus); \tag{B8}$$

(decuplet):

$$\phi^{S}_{\Delta^{++}} = uuu, \text{ etc.} \tag{B9}$$

$$\phi^{s}_{\Sigma^0} = \frac{1}{\sqrt{6}}(uds + dus + usd + dsu + sud + sdu), \text{ etc.}; \tag{B10}$$

(singlet):

$$\phi^{A}_{\Lambda} = \frac{1}{\sqrt{6}}(uds - dus - usd + dsu + sud - sdu); \tag{B11}$$

(uds type):

$$\phi_{\Lambda} = \frac{1}{\sqrt{2}}(ud - du)s, \qquad \phi_{\Sigma} = \frac{1}{\sqrt{2}}(ud + du)s; \tag{B12}$$

and the spin wave functions

$$\chi^{\rho}_{+} = \frac{1}{\sqrt{2}}(\uparrow\downarrow\uparrow - \downarrow\uparrow\uparrow), \tag{B13}$$

$$\chi^{\rho}_{-} = \frac{1}{\sqrt{2}}(\uparrow\downarrow\downarrow - \downarrow\uparrow\downarrow), \tag{B14}$$

$$\chi^{\lambda}_{+} = -\frac{1}{\sqrt{6}}(\uparrow\downarrow\uparrow + \downarrow\uparrow\uparrow - 2\uparrow\uparrow\downarrow), \tag{B15}$$

$$\chi^{\lambda}_{-} = \frac{1}{\sqrt{6}}(\uparrow\downarrow\downarrow + \downarrow\uparrow\downarrow - 2\downarrow\downarrow\uparrow), \tag{B16}$$

$$\chi^{s}_{3/2} = \uparrow\uparrow\uparrow, \text{ etc.} \tag{B17}$$

We explicitly display here only the top state of a given J^P multiplet, and we also display only the state of maximum J formed from coupling a given L and S; the states of smaller J were constructed using standard tables in the LS order. We have the octet states of the SU(6) type

$$|^{2}8(56',0^+)\tfrac{1}{2}^+\rangle = |8\,^2S_S\tfrac{1}{2}^+\rangle = \frac{1}{\sqrt{2}}(\chi^{\rho}_{+}\phi^{\rho} + \chi^{\lambda}_{+}\phi^{\lambda})\psi^{s\prime}_{00}\,, \tag{B18}$$

$$|^{2}8(70,0^+)\tfrac{1}{2}^+\rangle = |8\,^2S_M\tfrac{1}{2}^+\rangle = \tfrac{1}{2}(\chi^{\rho}_{+}\phi^{\rho}\psi^{\lambda}_{00} + \chi^{\rho}_{+}\phi^{\lambda}\psi^{\rho}_{00} + \chi^{\lambda}_{+}\phi^{\rho}\psi^{\rho}_{00} - \chi^{\lambda}_{+}\phi^{\lambda}\psi^{\lambda}_{00})\,, \tag{B19}$$

$$|^{4}8(70,0^+)\tfrac{3}{2}^+\rangle = |8\,^4S_M\tfrac{3}{2}^+\rangle = \chi^{s}_{3/2}\frac{1}{\sqrt{2}}(\phi^{\rho}\psi^{\rho}_{00} + \phi^{\lambda}\psi^{\lambda}_{00}), \tag{B20}$$

$$|^{2}8(56,2^+)\tfrac{5}{2}^+\rangle = |8\,^2D_S\tfrac{5}{2}^+\rangle = \frac{1}{\sqrt{2}}(\chi^{\rho}_{+}\phi^{\rho} + \chi^{\lambda}_{+}\phi^{\lambda})\psi^{s}_{22}\,, \tag{B21}$$

$$|^{2}8(70,2^+)\tfrac{5}{2}^+\rangle = |8\,^2D_M\tfrac{5}{2}^+\rangle = \tfrac{1}{2}(\chi^{\rho}_{+}\phi^{\rho}\psi^{\lambda}_{22} + \chi^{\rho}_{+}\phi^{\lambda}\psi^{\rho}_{22} + \chi^{\lambda}_{+}\phi^{\rho}\psi^{\rho}_{22} - \chi^{\lambda}_{+}\phi^{\lambda}\psi^{\lambda}_{22}), \tag{B22}$$

$$|^{4}8(70,2^+)\tfrac{7}{2}^+\rangle = |8\,^4D_M\tfrac{7}{2}^+\rangle = \chi^{s}_{3/2}\frac{1}{\sqrt{2}}(\phi^{\rho}\psi^{\rho}_{22} + \phi^{\lambda}\psi^{\lambda}_{22}), \tag{B23}$$

$$|^{2}8(20,1^+)\tfrac{3}{2}^+\rangle = |8\,^2P_A\tfrac{3}{2}^+\rangle = \frac{1}{\sqrt{2}}(\chi^{\rho}_{+}\phi^{\lambda} - \chi^{\lambda}_{+}\phi^{\rho})\psi^{\lambda}_{11}; \tag{B24}$$

the decuplet states of the SU(6) type

$$|^{4}10(56',0^+)\tfrac{3}{2}^+\rangle = |10\,^4S_S\tfrac{3}{2}^+\rangle = \chi^{s}_{3/2}\phi^{s}\psi^{s\prime}_{00}, \tag{B25}$$

$$|^{2}10(70,0^+)\tfrac{1}{2}^+\rangle = |10\,^2S_M\tfrac{1}{2}^+\rangle = \phi^{s}\frac{1}{\sqrt{2}}(\chi^{\rho}_{+}\psi^{\rho}_{00} + \chi^{\lambda}_{+}\psi^{\lambda}_{00}), \tag{B26}$$

$$|^{4}10(56,2^+)\tfrac{7}{2}^+\rangle = |10\,^4D_S\tfrac{7}{2}^+\rangle = \chi^{s}_{3/2}\phi^{s}\psi^{s}_{22}, \tag{B27}$$

$$|^{4}10(70,2^+)\tfrac{5}{2}^+\rangle = \phi^{s}\frac{1}{\sqrt{2}}\{\chi^{\rho}_{+}\psi^{\rho}_{22} + \chi^{\lambda}_{+}\psi^{\lambda}_{22}\}; \tag{B28}$$

the singlet states of the SU(6) type

$$|^{2}1(70,0^+)\tfrac{1}{2}^+\rangle = |1\,^2S_M\tfrac{1}{2}^+\rangle = \phi^{A}\frac{1}{\sqrt{2}}(\chi^{\rho}_{+}\psi^{\lambda}_{00} - \chi^{\lambda}_{+}\psi^{\rho}_{00}), \tag{B29}$$

$$|^{2}1(70,2^+)\tfrac{1}{2}^+\rangle = |1\,^2D_M\tfrac{5}{2}^+\rangle = \phi^{A}\frac{1}{\sqrt{2}}(\chi^{\rho}_{+}\psi^{\lambda}_{22} - \chi^{\lambda}_{+}\psi^{\rho}_{22}), \tag{B30}$$

$$|^{4}1(20,1^+)\tfrac{5}{2}^+\rangle = |1\,^4P_A\tfrac{5}{2}^+\rangle = \chi^{s}_{3/2}\phi^{A}\psi^{\lambda}_{11}; \tag{B31}$$

the uds-type Λ states

$$|\Lambda\,^2S_{\lambda\lambda}\tfrac{1}{2}^+\rangle = \phi_{\Lambda}\chi^{\rho}_{+}\psi^{\lambda\lambda}_{00}\,, \tag{B32}$$

$$|\Lambda\,^2S_{\rho\rho}\tfrac{1}{2}^+\rangle = \phi_{\Lambda}\chi^{\rho}_{+}\psi^{\rho\rho}_{00}\,, \tag{B33}$$

$$|\Lambda\,^2S_{\rho\lambda}\tfrac{1}{2}^+\rangle = \phi_{\Lambda}\chi^{\lambda}_{+}\psi^{\rho\lambda}_{00}\,, \tag{B34}$$

$$|\Lambda\,^2D_{\lambda\lambda}\tfrac{5}{2}^+\rangle = \phi_{\Lambda}\chi^{\rho}_{+}\psi^{\lambda\lambda}_{22}\,, \tag{B35}$$

$$|\Lambda\,^2D_{\rho\rho}\tfrac{5}{2}^+\rangle = \phi_{\Lambda}\chi^{\rho}_{+}\psi^{\rho\rho}_{22}, \tag{B36}$$

$$|\Lambda^2 D_{\rho\lambda}\tfrac{5}{2}^+\rangle = \phi_\Lambda \chi_+^\lambda \psi_{22}^{\rho\lambda}, \tag{B37}$$

$$|\Lambda^2 P_{\rho\lambda}\tfrac{3}{2}^+\rangle = \phi_\Lambda \chi_+^\lambda \psi_{11}^{\rho\lambda}, \tag{B38}$$

$$|\Lambda^4 S_{\rho\lambda}\tfrac{3}{2}^+\rangle = \phi_\Lambda \chi_{3/2}^s \psi_{00}^{\rho\lambda}, \tag{B39}$$

$$|\Lambda^4 D_{\rho\lambda}\tfrac{7}{2}^+\rangle = \phi_\Lambda \chi_{3/2}^s \psi_{22}^{\rho\lambda}, \tag{B40}$$

$$|\Lambda^4 P_{\rho\lambda}\tfrac{5}{2}^+\rangle = \phi_\Lambda \chi_{3/2}^s \psi_{11}^{\rho\lambda}; \tag{B41}$$

and the *uds*-type Σ states

$$|\Sigma^2 S_{\lambda\lambda}\tfrac{1}{2}^+\rangle = \phi_\Sigma \chi_+^\lambda \psi_{00}^{\lambda\lambda}, \tag{B42}$$

$$|\Sigma^2 S_{\rho\rho}\tfrac{1}{2}^+\rangle = \phi_\Sigma \chi_+^\lambda \psi_{00}^{\rho\rho}, \tag{B43}$$

$$|\Sigma^2 S_{\rho\lambda}\tfrac{1}{2}^+\rangle = \phi_\Sigma \chi_+^\rho \psi_{00}^{\rho\lambda}, \tag{B44}$$

$$|\Sigma^2 D_{\lambda\lambda}\tfrac{5}{2}^+\rangle = \phi_\Sigma \chi_+^\lambda \psi_{22}^{\lambda\lambda}, \tag{B45}$$

$$|\Sigma^2 D_{\rho\rho}\tfrac{5}{2}^+\rangle = \phi_\Sigma \chi_+^\lambda \psi_{22}^{\rho\rho}, \tag{B46}$$

$$|\Sigma^2 D_{\rho\lambda}\tfrac{5}{2}^+\rangle = \phi_\Sigma \chi_+^\rho \psi_{22}^{\rho\lambda}, \tag{B47}$$

$$|\Sigma^2 P_{\rho\lambda}\tfrac{3}{2}^+\rangle = \phi_\Sigma \chi_+^\rho \psi_{11}^{\rho\lambda}, \tag{B48}$$

$$|\Sigma^4 S_{\lambda\lambda}\tfrac{3}{2}^+\rangle = \phi_\Sigma \chi_{3/2}^s \psi_{00}^{\lambda\lambda}, \tag{B49}$$

$$|\Sigma^4 S_{\rho\rho}\tfrac{3}{2}^+\rangle = \phi_\Sigma \chi_{3/2}^s \psi_{00}^{\rho\rho}, \tag{B50}$$

$$|\Sigma^4 D_{\lambda\lambda}\tfrac{7}{2}^+\rangle = \phi_\Sigma \chi_{3/2}^s \psi_{22}^{\lambda\lambda}, \tag{B51}$$

$$|\Sigma^4 D_{\rho\rho}\tfrac{7}{2}^+\rangle = \phi_\Sigma \chi_{3/2}^s \psi_{22}^{\rho\rho}. \tag{B52}$$

Finally, the relation between the SU(6) and *uds* bases is that

$$|\Lambda^2 L_{\lambda\lambda}\rangle \longleftrightarrow \frac{1}{\sqrt{2}}|\Lambda_8{}^2L_S\rangle - \tfrac{1}{2}|\Lambda_8{}^2L_M\rangle + \tfrac{1}{2}|\Lambda_1{}^2L_M\rangle, \tag{B53}$$

$$|\Lambda^2 L_{\rho\lambda}\rangle \longleftrightarrow \frac{1}{\sqrt{2}}|\Lambda_8{}^2L_M\rangle + \frac{1}{\sqrt{2}}|\Lambda_1{}^2L_M\rangle, \tag{B54}$$

$$|\Lambda^2 L_{\rho\rho}\rangle \longleftrightarrow \frac{1}{\sqrt{2}}|\Lambda_8{}^2L_S\rangle + \tfrac{1}{2}|\Lambda_8{}^2L_M\rangle - \tfrac{1}{2}|\Lambda_1{}^2L_M\rangle, \tag{B55}$$

$$|\Lambda^4 L_{\rho\lambda}\rangle \longleftrightarrow |\Lambda_8{}^4L_M\rangle, \tag{B56}$$

for $L = S$ or D and

$$|\Lambda^2 P_{\rho\lambda}\rangle \longleftrightarrow -|\Lambda_8{}^2P_A\rangle, \tag{B57}$$

$$|\Lambda^4 P_{\rho\lambda}\rangle \longleftrightarrow -|\Lambda_1{}^4P_A\rangle, \tag{B58}$$

while

$$|\Sigma^2 L_{\lambda\lambda}\rangle \longleftrightarrow \frac{1}{\sqrt{2}}|\Sigma_8{}^2L_S\rangle + \tfrac{1}{2}|\Sigma_8{}^2L_M\rangle - \tfrac{1}{2}|\Sigma_{10}{}^2L_M\rangle, \tag{B59}$$

$$|\Sigma^2 L_{\rho\lambda}\rangle \longleftrightarrow \frac{1}{\sqrt{2}}|\Sigma_8{}^2L_M\rangle + \frac{1}{\sqrt{2}}|\Sigma_{10}{}^2L_M\rangle, \tag{B60}$$

$$|\Sigma^2 L_{\rho\rho}\rangle \longleftrightarrow \frac{1}{\sqrt{2}}|\Sigma_8{}^2L_S\rangle - \tfrac{1}{2}|\Sigma_8{}^2L_M\rangle + \tfrac{1}{2}|\Sigma_{10}{}^2L_M\rangle, \tag{B61}$$

$$|\Sigma^4 L_{\lambda\lambda}\rangle \longleftrightarrow -\frac{1}{\sqrt{2}}|\Sigma_8{}^4L_M\rangle + \frac{1}{\sqrt{2}}|\Sigma_{10}{}^4L_S\rangle, \tag{B62}$$

$$|\Sigma^4 L_{\rho\rho}\rangle \longleftrightarrow \frac{1}{\sqrt{2}}|\Sigma_8{}^4L_M\rangle + \frac{1}{\sqrt{2}}|\Sigma_{10}{}^4L_S\rangle, \tag{B63}$$

for $L = S$ or D and

$$|\Sigma^2 P_{\rho\lambda}\rangle \longleftrightarrow |\Sigma^2 P_A\rangle, \tag{B64}$$

where these correspondences are to be interpreted to mean that matrix elements between two states on the left will be equal to matrix elements between the two corresponding states on the right.

APPENDIX C: THE HYPERFINE MATRIX ELEMENTS

Some general features of the calculation of the hyperfine matrix elements having been described in Sec. III, we confine ourselves here to some details and to the tabulation of the results.

The matrix elements in the nonstrange sector are really quite straightforward, especially the contact terms:

$$\tilde{H}^{12}_{\text{contact}} = \frac{4\sqrt{2}\,\pi\alpha_s}{9m_d{}^2}\vec{S}_1\cdot\vec{S}_2\delta^3(\vec{\rho}), \tag{C1}$$

but also the tensor terms:

$$\tilde{H}^{12}_{\text{tensor}} = \frac{\alpha_s}{\sqrt{2}\,m_d{}^2\rho^5}\big[\tfrac{1}{4}S_{1-}S_{2-}\rho_+^2 + \tfrac{1}{2}(S_{1-}S_{2_z} + S_{1_z}S_{2-})\rho_+\rho_z + \tfrac{1}{12}(S_{1+}S_{2-} + S_{1-}S_{2+} - 4S_{1_z}S_{2_z})(\rho^2 - 3\rho_z{}^2)$$
$$+ \tfrac{1}{2}(S_{1+}S_{2_z} + S_{1_z}S_{2+})\rho_-\rho_z + \tfrac{1}{4}S_{1+}S_{2+}\rho_-^2\big], \tag{C2}$$

although the tensor terms may be computed much more simply by the use of Racah coefficients. In any event one obtains the matrices given in Table VII.

The matrix elements in the $S = -1$ sector may most easily be evaluated using a trick. If we write

$$H_{\text{hyp}} = \sum_{i<j}[1 - (1-x)(\delta_{is} + \delta_{js})]\tilde{H}^{ij}_{\text{hyp}}, \tag{C3}$$

where δ_{is} equals one or zero depending on whether quark i is strange or nonstrange, then in the SU(6) basis one can apply formula (49). Since

$$\langle\phi_\Lambda^\rho|(\delta_{1s} + \delta_{2s})|\phi_\Lambda^\rho\rangle = \tfrac{1}{3}, \tag{C4}$$

$$\langle\phi_\Sigma^\rho|(\delta_{1s} + \delta_{2s})|\phi_\Sigma^\rho\rangle = 1, \tag{C5}$$

$$\langle\phi_\Lambda^A|\delta_{1s} + \delta_{2s}|\phi_\Lambda^A\rangle = \tfrac{2}{3}, \tag{C6}$$

TABLE VII. Hyperfine matrix elements in the $S=0$ sector (in units of δ).

	H_{contact}	H_{tensor}
${}^4N(70,2^+)\frac{7}{2}^+$	$+\frac{1}{8}$	$-\frac{9}{140}$
${}^4\Delta(56,2^+)\frac{7}{2}^+$	$+\frac{1}{4}$	$-\frac{1}{35}$
${}^2N(56,2^+)\frac{5}{2}^+$ ${}^2N(70,2^+)\frac{5}{2}^+$ ${}^4N(70,2^+)\frac{5}{2}^+$	$\begin{bmatrix} -\frac{1}{4} & +\frac{\sqrt{2}}{4} & 0 \\ +\frac{\sqrt{2}}{4} & -\frac{1}{8} & 0 \\ 0 & 0 & +\frac{1}{8} \end{bmatrix}$	$\begin{bmatrix} 0 & 0 & -\frac{\sqrt{14}}{140} \\ 0 & 0 & -\frac{\sqrt{7}}{56} \\ -\frac{\sqrt{14}}{140} & -\frac{\sqrt{7}}{56} & +\frac{9}{56} \end{bmatrix}$
${}^4\Delta(56,2^+)\frac{5}{2}^+$ ${}^2\Delta(70,2^+)\frac{5}{2}^+$	$\begin{bmatrix} +\frac{1}{4} & 0 \\ 0 & +\frac{1}{8} \end{bmatrix}$	$\begin{bmatrix} +\frac{1}{14} & -\frac{\sqrt{7}}{70} \\ -\frac{\sqrt{7}}{70} & 0 \end{bmatrix}$
${}^4N(70,0^+)\frac{3}{2}^+$ ${}^2N(56,2^+)\frac{3}{2}^+$ ${}^2N(70,2^+)\frac{3}{2}^+$ ${}^4N(70,2^+)\frac{3}{2}^+$ ${}^2N(20,1^+)\frac{3}{2}^+$	$\begin{bmatrix} +\frac{5}{16} & 0 & 0 & 0 & 0 \\ 0 & -\frac{1}{4} & +\frac{\sqrt{2}}{4} & 0 & 0 \\ 0 & +\frac{\sqrt{2}}{4} & -\frac{1}{8} & 0 & 0 \\ 0 & 0 & 0 & +\frac{1}{8} & 0 \\ 0 & 0 & 0 & 0 & 0 \end{bmatrix}$	$\begin{bmatrix} 0 & +\frac{\sqrt{10}}{80} & -\frac{\sqrt{5}}{16} & +\frac{3\sqrt{10}}{80} & 0 \\ +\frac{\sqrt{10}}{80} & 0 & 0 & +\frac{1}{20} & 0 \\ -\frac{\sqrt{5}}{16} & 0 & 0 & +\frac{\sqrt{2}}{16} & 0 \\ +\frac{3\sqrt{10}}{80} & +\frac{1}{20} & +\frac{\sqrt{2}}{16} & 0 & +\frac{3\sqrt{5}}{40} \\ 0 & 0 & 0 & +\frac{3\sqrt{5}}{40} & 0 \end{bmatrix}$
${}^4\Delta(56',0^+)\frac{3}{2}^+$ ${}^4\Delta(56,2^+)\frac{3}{2}^+$ ${}^2\Delta(70,2^+)\frac{3}{2}^+$	$\begin{bmatrix} +\frac{5}{8} & 0 & 0 \\ 0 & +\frac{1}{4} & 0 \\ 0 & 0 & +\frac{1}{8} \end{bmatrix}$	$\begin{bmatrix} 0 & -\frac{\sqrt{10}}{40} & +\frac{\sqrt{5}}{40} \\ -\frac{\sqrt{10}}{40} & 0 & +\frac{\sqrt{2}}{20} \\ +\frac{\sqrt{5}}{40} & +\frac{\sqrt{2}}{20} & 0 \end{bmatrix}$
${}^2N(56',0^+)\frac{1}{2}^+$ ${}^2N(70,0^+)\frac{1}{2}^+$ ${}^4N(70,2^+)\frac{1}{2}^+$ ${}^2N(20,1^+)\frac{1}{2}^+$	$\begin{bmatrix} -\frac{5}{8} & -\frac{\sqrt{2}}{8} & 0 & 0 \\ -\frac{\sqrt{2}}{8} & -\frac{5}{16} & 0 & 0 \\ 0 & 0 & +\frac{1}{8} & 0 \\ 0 & 0 & 0 & 0 \end{bmatrix}$	$\begin{bmatrix} 0 & 0 & -\frac{\sqrt{5}}{40} & 0 \\ 0 & 0 & +\frac{\sqrt{10}}{16} & 0 \\ -\frac{\sqrt{5}}{40} & +\frac{\sqrt{10}}{16} & -\frac{9}{40} & -\frac{3\sqrt{10}}{40} \\ 0 & 0 & -\frac{3\sqrt{10}}{40} & 0 \end{bmatrix}$
${}^2\Delta(70,0^+)\frac{1}{2}^+$ ${}^4\Delta(56,2^+)\frac{1}{2}^+$	$\begin{bmatrix} +\frac{5}{16} & 0 \\ 0 & +\frac{1}{4} \end{bmatrix}$	$\begin{bmatrix} 0 & -\frac{\sqrt{10}}{40} \\ -\frac{\sqrt{10}}{40} & -\frac{1}{10} \end{bmatrix}$

TABLE VIII. Matrix elements of the contact term in the $S=-1$ sector in the SU(6) basis (in units of δ).

$$\Lambda_8{}^4D_M\tfrac{7}{2}^+ \qquad +\frac{1}{8}x$$

$$\begin{array}{l} \Sigma_{10}{}^4D_S\tfrac{7}{2}^+ \\[6pt] \Sigma_8{}^4D_M\tfrac{7}{2}^+ \end{array} \begin{bmatrix} +\frac{1}{4}\left(\frac{1+2x}{3}\right) & -\frac{1}{12}(1-x) \\ -\frac{1}{12}(1-x) & +\frac{1}{8}\left(\frac{2+x}{3}\right) \end{bmatrix}$$

$$\begin{array}{l} \Lambda_8{}^2D_S\tfrac{5}{2}^+ \\[6pt] \Lambda_1{}^2D_M\tfrac{5}{2}^+ \\[6pt] \Lambda_8{}^2D_M\tfrac{5}{2}^+ \\[6pt] \Lambda_8{}^4D_M\tfrac{5}{2}^+ \\[6pt] \Lambda_1{}^4P_A\tfrac{5}{2}^+ \end{array} \begin{bmatrix} -\frac{1}{4} & -\frac{\sqrt{2}}{8}(1-x) & +\frac{\sqrt{2}}{4}\left(\frac{1+x}{2}\right) & 0 & 0 \\ -\frac{\sqrt{2}}{8}(1-x) & -\frac{3}{8}\left(\frac{1+2x}{3}\right) & +\frac{1}{8}(1-x) & 0 & 0 \\ +\frac{\sqrt{2}}{4}\left(\frac{1+x}{2}\right) & +\frac{1}{8}(1-x) & -\frac{1}{8} & 0 & 0 \\ 0 & 0 & 0 & +\frac{1}{8}x & 0 \\ 0 & 0 & 0 & 0 & 0 \end{bmatrix}$$

$$\begin{array}{l} \Sigma_8{}^2D_S\tfrac{5}{2}^+ \\[6pt] \Sigma_{10}{}^4D_S\tfrac{5}{2}^+ \\[6pt] \Sigma_8{}^2D_M\tfrac{5}{2}^+ \\[6pt] \Sigma_8{}^4D_M\tfrac{5}{2}^+ \\[6pt] \Sigma_{10}{}^2D_M\tfrac{5}{2}^+ \end{array} \begin{bmatrix} -\frac{1}{4}\left(\frac{4x-1}{3}\right) & 0 & +\frac{\sqrt{2}}{4}\left(\frac{5x+1}{6}\right) & 0 & -\frac{\sqrt{2}}{24}(1-x) \\ 0 & +\frac{1}{4}\left(\frac{1+2x}{3}\right) & 0 & -\frac{1}{12}(1-x) & 0 \\ +\frac{\sqrt{2}}{4}\left(\frac{5x+1}{6}\right) & 0 & -\frac{1}{8}\left(\frac{4x-1}{3}\right) & 0 & -\frac{1}{24}(1-x) \\ 0 & -\frac{1}{12}(1-x) & 0 & +\frac{1}{8}\left(\frac{2+x}{3}\right) & 0 \\ -\frac{\sqrt{2}}{24}(1-x) & 0 & -\frac{1}{24}(1-x) & 0 & +\frac{1}{8}\left(\frac{1+2x}{3}\right) \end{bmatrix}$$

$$\begin{array}{l} \Lambda_8{}^4S_M\tfrac{3}{2}^+ \\[6pt] \Lambda_8{}^2D_S\tfrac{3}{2}^+ \\[6pt] \Lambda_1{}^2D_M\tfrac{3}{2}^+ \\[6pt] \Lambda_8{}^2D_M\tfrac{3}{2}^+ \\[6pt] \Lambda_8{}^4D_M\tfrac{3}{2}^+ \\[6pt] \Lambda_1{}^4P_A\tfrac{3}{2}^+ \\[6pt] \Lambda_8{}^2P_A\tfrac{3}{2}^+ \end{array} \begin{bmatrix} +\frac{5}{16}x & 0 & 0 & 0 & 0 & 0 & 0 \\ 0 & -\frac{1}{4} & -\frac{\sqrt{2}}{8}(1-x) & +\frac{\sqrt{2}}{4}\left(\frac{1+x}{2}\right) & 0 & 0 & 0 \\ 0 & -\frac{\sqrt{2}}{8}(1-x) & -\frac{3}{8}\left(\frac{1+2x}{3}\right) & +\frac{1}{8}(1-x) & 0 & 0 & 0 \\ 0 & +\frac{\sqrt{2}}{4}\left(\frac{1+x}{2}\right) & +\frac{1}{8}(1-x) & -\frac{1}{8} & 0 & 0 & 0 \\ 0 & 0 & 0 & 0 & +\frac{1}{8}x & 0 & 0 \\ 0 & 0 & 0 & 0 & 0 & 0 & 0 \\ 0 & 0 & 0 & 0 & 0 & 0 & 0 \end{bmatrix}$$

TABLE VIII. (*Continued*)

$\Sigma_{10}{}^4S_S\frac{3}{2}^+$	$+\frac{5}{8}\left(\frac{1+2x}{3}\right)$	$+\frac{1}{24}(1-x)$	0	0	0	0	0	0
$\Sigma_8{}^4S_M\frac{3}{2}^+$	$+\frac{1}{24}(1-x)$	$+\frac{5}{16}\left(\frac{2+x}{3}\right)$	0	0	0	0	0	0
$\Sigma_8{}^2D_S\frac{3}{2}^+$	0	0	$-\frac{1}{4}\left(\frac{4x-1}{3}\right)$	0	$+\frac{\sqrt{2}}{4}\left(\frac{5x+1}{6}\right)$	0	$-\frac{\sqrt{2}}{24}(1-x)$	0
$\Sigma_{10}{}^4D_S\frac{3}{2}^+$	0	0	0	$+\frac{1}{4}\left(\frac{1+2x}{3}\right)$	0	$-\frac{1}{12}(1-x)$	0	0
$\Sigma_8{}^2D_M\frac{3}{2}^+$	0	0	$+\frac{\sqrt{2}}{4}\left(\frac{5x+1}{6}\right)$	0	$-\frac{1}{8}\left(\frac{4x-1}{3}\right)$	0	$-\frac{1}{24}(1-x)$	0
$\Sigma_8{}^4D_M\frac{3}{2}^+$	0	0	0	$-\frac{1}{12}(1-x)$	0	$+\frac{1}{8}\left(\frac{2+x}{3}\right)$	0	0
$\Sigma_{10}{}^2D_M\frac{3}{2}^+$	0	0	$-\frac{\sqrt{2}}{24}(1-x)$	0	$-\frac{1}{24}(1-x)$	0	$+\frac{1}{8}\left(\frac{1+2x}{3}\right)$	0
$\Sigma_8{}^2P_A\frac{3}{2}^+$	0	0	0	0	0	0	0	0

$\Lambda_8{}^2S_S\frac{1}{2}^+$	$-\frac{5}{8}$	$-\frac{\sqrt{2}}{8}\left(\frac{1+x}{2}\right)$	$+\frac{\sqrt{2}}{16}(1-x)$	0	0
$\Lambda_8{}^2S_M\frac{1}{2}^+$	$-\frac{\sqrt{2}}{8}\left(\frac{1+x}{2}\right)$	$-\frac{5}{16}$	$+\frac{5}{16}(1-x)$	0	0
$\Lambda_1{}^2S_M\frac{1}{2}^+$	$+\frac{\sqrt{2}}{16}(1-x)$	$+\frac{5}{16}(1-x)$	$-\frac{15}{16}\left(\frac{1+2x}{3}\right)$	0	0
$\Lambda_8{}^4D_M\frac{1}{2}^+$	0	0	0	$+\frac{1}{8}x$	0
$\Lambda_1{}^4P_A\frac{1}{2}^+$	0	0	0	0	0
$\Lambda_8{}^2P_A\frac{1}{2}^+$	0	0	0	0	0

$\Sigma_8{}^2S_S\frac{1}{2}^+$	$-\frac{5}{8}\left(\frac{4x-1}{3}\right)$	$-\frac{\sqrt{2}}{8}\left(\frac{5x+1}{6}\right)$	$+\frac{\sqrt{2}}{48}(1-x)$	0	0	0
$\Sigma_8{}^2S_M\frac{1}{2}^+$	$-\frac{\sqrt{2}}{8}\left(\frac{5x+1}{6}\right)$	$-\frac{5}{16}\left(\frac{4x-1}{3}\right)$	$-\frac{5}{48}(1-x)$	0	0	0
$\Sigma_{10}{}^2S_M\frac{1}{2}^+$	$+\frac{\sqrt{2}}{48}(1-x)$	$-\frac{5}{48}(1-x)$	$+\frac{5}{16}\left(\frac{1+2x}{3}\right)$	0	0	0
$\Sigma_{10}{}^4D_S\frac{1}{2}^+$	0	0	0	$+\frac{1}{4}\left(\frac{1+2x}{3}\right)$	$-\frac{1}{12}(1-x)$	0
$\Sigma_8{}^4D_M\frac{1}{2}^+$	0	0	0	$-\frac{1}{12}(1-x)$	$+\frac{1}{8}\left(\frac{2+x}{3}\right)$	0
$\Sigma_8{}^2P_A\frac{1}{2}^+$	0	0	0	0	0	0

TABLE IX. Matrix elements of the tensor term in the $S=-1$ sector in the SU(6) basis (in units of δ).

$\Lambda_8{}^4D_M\frac{7}{2}^+$	$-\frac{9}{140}\left(\frac{14+13x}{27}\right)$				
$\Sigma_{10}{}^4D_S\frac{7}{2}^+$	$-\frac{1}{35}\left(\frac{1+2x}{3}\right)$	$-\frac{1}{105}(1-x)$			
$\Sigma_8{}^4D_M\frac{7}{2}^+$	$-\frac{1}{105}(1-x)$	$-\frac{9}{140}\left(\frac{4+23x}{27}\right)$			
$\Lambda_8{}^2D_S\frac{5}{2}^+$	0	0	0	$-\frac{\sqrt{14}}{140}x$	0
$\Lambda_1{}^2D_M\frac{5}{2}^+$	0	0	0	$-\frac{\sqrt{7}}{60}(1-x)$	$-\frac{\sqrt{3}}{20}\left(\frac{1+2x}{3}\right)$
$\Lambda_8{}^2D_M\frac{5}{2}^+$	0	0	0	$-\frac{\sqrt{7}}{56}\left(\frac{14+x}{15}\right)$	$-\frac{\sqrt{3}}{60}(1-x)$
$\Lambda_8{}^4D_M\frac{5}{2}^+$	$-\frac{\sqrt{14}}{140}x$	$-\frac{\sqrt{7}}{60}(1-x)$	$-\frac{\sqrt{7}}{56}\left(\frac{14+x}{15}\right)$	$+\frac{9}{56}\left(\frac{14+13x}{27}\right)$	$+\frac{\sqrt{21}}{60}(1-x)$
$\Lambda_1{}^4P_A\frac{5}{2}^+$	0	$-\frac{\sqrt{3}}{20}\left(\frac{1+2x}{3}\right)$	$-\frac{\sqrt{3}}{60}(1-x)$	$+\frac{\sqrt{21}}{60}(1-x)$	$+\frac{1}{20}\left(\frac{1+2x}{3}\right)$
$\Sigma_8{}^2D_S\frac{5}{2}^+$	0	$-\frac{\sqrt{14}}{210}(1-x)$	0	$-\frac{\sqrt{14}}{140}\left(\frac{2+x}{3}\right)$	0
$\Sigma_{10}{}^4D_S\frac{5}{2}^+$	$-\frac{\sqrt{14}}{210}(1-x)$	$+\frac{1}{14}\left(\frac{1+2x}{3}\right)$	$+\frac{\sqrt{7}}{210}(1-x)$	$+\frac{1}{42}(1-x)$	$-\frac{\sqrt{7}}{70}\left(\frac{1+2x}{3}\right)$
$\Sigma_8{}^2D_M\frac{5}{2}^+$	0	$+\frac{\sqrt{7}}{210}(1-x)$	0	$-\frac{\sqrt{7}}{56}\left(\frac{19x-4}{15}\right)$	0
$\Sigma_8{}^4D_M\frac{5}{2}^+$	$-\frac{\sqrt{14}}{140}\left(\frac{2+x}{3}\right)$	$+\frac{1}{42}(1-x)$	$-\frac{\sqrt{7}}{56}\left(\frac{19x-4}{15}\right)$	$+\frac{9}{56}\left(\frac{4+23x}{27}\right)$	$-\frac{\sqrt{7}}{210}(1-x)$
$\Sigma_{10}{}^2D_M\frac{5}{2}^+$	0	$-\frac{\sqrt{7}}{70}\left(\frac{1+2x}{3}\right)$	0	$-\frac{\sqrt{7}}{210}(1-x)$	0

TABLE IX. (*Continued*)

$\Lambda_8{}^4S_M\frac{3}{2}^+$	0	$+\frac{\sqrt{10}}{80}x$	$-\frac{\sqrt{5}}{30}(1-x)$	$-\frac{\sqrt{5}}{16}\left(\frac{8+7x}{15}\right)$	$+\frac{3\sqrt{10}}{80}\left(\frac{8+x}{9}\right)$	0	0
$\Lambda_8{}^2D_S\frac{3}{2}^+$	$+\frac{\sqrt{10}}{80}x$	0	0	0	$+\frac{1}{20}x$	0	0
$\Lambda_1{}^2D_M\frac{3}{2}^+$	$-\frac{\sqrt{5}}{30}(1-x)$	0	0	0	$+\frac{7\sqrt{2}}{120}(1-x)$	$-\frac{9\sqrt{2}}{40}\left(\frac{1+2x}{3}\right)$	0
$\Lambda_8{}^2D_M\frac{3}{2}^+$	$-\frac{\sqrt{5}}{16}\left(\frac{8+7x}{15}\right)$	0	0	0	$+\frac{\sqrt{2}}{16}\left(\frac{14+x}{15}\right)$	$+\frac{3\sqrt{2}}{40}(1-x)$	0
$\Lambda_8{}^4D_M\frac{3}{2}^+$	$+\frac{3\sqrt{10}}{80}\left(\frac{8+x}{9}\right)$	$+\frac{1}{20}x$	$+\frac{7\sqrt{2}}{120}(1-x)$	$+\frac{\sqrt{2}}{16}\left(\frac{14+x}{15}\right)$	0	$+\frac{1}{10}(1-x)$	$+\frac{3\sqrt{5}}{40}\left(\frac{2+x}{3}\right)$
$\Lambda_1{}^4P_A\frac{3}{2}^+$	0	0	$-\frac{9\sqrt{2}}{40}\left(\frac{1+2x}{3}\right)$	$+\frac{3\sqrt{2}}{40}(1-x)$	$+\frac{1}{10}(1-x)$	$-\frac{1}{5}\left(\frac{1+2x}{3}\right)$	$+\frac{\sqrt{5}}{60}(1-x)$
$\Lambda_8{}^2P_A\frac{3}{2}^+$	0	0	0	0	$+\frac{3\sqrt{5}}{40}\left(\frac{2+x}{3}\right)$	$+\frac{\sqrt{5}}{60}(1-x)$	0

$\Sigma_{10}{}^4S_S\frac{3}{2}^+$	0	0	$+\frac{\sqrt{10}}{120}(1-x)$	$-\frac{\sqrt{10}}{40}\left(\frac{1+2x}{3}\right)$	$-\frac{\sqrt{5}}{120}(1-x)$	$-\frac{\sqrt{10}}{120}(1-x)$	$+\frac{\sqrt{5}}{40}\left(\frac{1+2x}{3}\right)$	0
$\Sigma_8{}^4S_M\frac{3}{2}^+$	0	0	$+\frac{\sqrt{10}}{80}\left(\frac{2+x}{3}\right)$	$-\frac{\sqrt{10}}{120}(1-x)$	$-\frac{\sqrt{5}}{16}\left(\frac{2+13x}{15}\right)$	$+\frac{3\sqrt{10}}{80}\left(\frac{11x-2}{9}\right)$	$+\frac{\sqrt{5}}{120}(1-x)$	0
$\Sigma_8{}^2D_S\frac{3}{2}^+$	$+\frac{\sqrt{10}}{120}(1-x)$	$+\frac{\sqrt{10}}{80}\left(\frac{2+x}{3}\right)$	0	$+\frac{1}{30}(1-x)$	0	$+\frac{1}{20}\left(\frac{2+x}{3}\right)$	0	0
$\Sigma_{10}{}^4D_S\frac{3}{2}^+$	$-\frac{\sqrt{10}}{40}\left(\frac{1+2x}{3}\right)$	$-\frac{\sqrt{10}}{120}(1-x)$	$+\frac{1}{30}(1-x)$	0	$-\frac{\sqrt{2}}{60}(1-x)$	0	$+\frac{\sqrt{2}}{20}\left(\frac{1+2x}{3}\right)$	0
$\Sigma_8{}^2D_M\frac{3}{2}^+$	$-\frac{\sqrt{5}}{120}(1-x)$	$-\frac{\sqrt{5}}{16}\left(\frac{2+13x}{15}\right)$	0	$-\frac{\sqrt{2}}{60}(1-x)$	0	$+\frac{\sqrt{2}}{16}\left(\frac{19x-4}{15}\right)$	0	0
$\Sigma_8{}^4D_M\frac{3}{2}^+$	$-\frac{\sqrt{10}}{120}(1-x)$	$+\frac{3\sqrt{10}}{80}\left(\frac{11x-2}{9}\right)$	$+\frac{1}{20}\left(\frac{2+x}{3}\right)$	0	$+\frac{\sqrt{2}}{16}\left(\frac{19x-4}{15}\right)$	0	$+\frac{\sqrt{2}}{60}(1-x)$	$+\frac{3\sqrt{5}}{40}x$
$\Sigma_{10}{}^2D_M\frac{3}{2}^+$	$+\frac{\sqrt{5}}{40}\left(\frac{1+2x}{3}\right)$	$+\frac{\sqrt{5}}{120}(1-x)$	0	$+\frac{\sqrt{2}}{20}\left(\frac{1+2x}{3}\right)$	0	$+\frac{\sqrt{2}}{60}(1-x)$	0	0
$\Sigma_8{}^2P_A\frac{3}{2}^+$	0	0	0	0	0	$+\frac{3\sqrt{5}}{40}x$	0	0

TABLE IX. (*Continued*)

$\Lambda_8{}^2S_S\frac{1}{2}^+$	0	0	0	$-\frac{\sqrt{5}}{40}x$	0	0
$\Lambda_8{}^2S_M\frac{1}{2}^+$	0	0	0	$+\frac{\sqrt{10}}{16}\left(\frac{8+7x}{15}\right)$	0	0
$\Lambda_1{}^2S_M\frac{1}{2}^+$	0	0	0	$+\frac{\sqrt{10}}{30}(1-x)$	0	0
$\Lambda_8{}^4D_M\frac{1}{2}^+$	$-\frac{\sqrt{5}}{40}x$	$+\frac{\sqrt{10}}{16}\left(\frac{8+7x}{15}\right)$	$+\frac{\sqrt{10}}{30}(1-x)$	$-\frac{9}{40}\left(\frac{14+13x}{27}\right)$	$-\frac{\sqrt{5}}{20}(1-x)$	$-\frac{3\sqrt{10}}{40}\left(\frac{2+x}{3}\right)$
$\Lambda_1{}^4P_A\frac{1}{2}^+$	0	0	0	$-\frac{\sqrt{5}}{20}(1-x)$	$+\frac{1}{4}\left(\frac{1+2x}{3}\right)$	$-\frac{\sqrt{2}}{12}(1-x)$
$\Lambda_8{}^2P_A\frac{1}{2}^+$	0	0	0	$-\frac{3\sqrt{10}}{40}\left(\frac{2+x}{3}\right)$	$-\frac{\sqrt{2}}{12}(1-x)$	0

$\Sigma_8{}^2S_S\frac{1}{2}^+$	0	0	0	$-\frac{\sqrt{5}}{60}(1-x)$	$-\frac{\sqrt{5}}{40}\left(\frac{2+x}{3}\right)$	0
$\Sigma_8{}^2S_M\frac{1}{2}^+$	0	0	0	$+\frac{\sqrt{10}}{120}(1-x)$	$+\frac{\sqrt{10}}{16}\left(\frac{13x+2}{15}\right)$	0
$\Sigma_{10}{}^2S_M\frac{1}{2}^+$	0	0	0	$-\frac{\sqrt{10}}{40}\left(\frac{1+2x}{3}\right)$	$-\frac{\sqrt{10}}{120}(1-x)$	0
$\Sigma_{10}{}^4D_S\frac{1}{2}^+$	$-\frac{\sqrt{5}}{60}(1-x)$	$+\frac{\sqrt{10}}{120}(1-x)$	$-\frac{\sqrt{10}}{40}\left(\frac{1+2x}{3}\right)$	$-\frac{1}{10}\left(\frac{1+2x}{3}\right)$	$-\frac{1}{30}(1-x)$	0
$\Sigma_8{}^4D_M\frac{1}{2}^+$	$-\frac{\sqrt{5}}{40}\left(\frac{2+x}{3}\right)$	$+\frac{\sqrt{10}}{16}\left(\frac{13x+2}{15}\right)$	$-\frac{\sqrt{10}}{120}(1-x)$	$-\frac{1}{30}(1-x)$	$-\frac{9}{40}\left(\frac{4+23x}{27}\right)$	$-\frac{3\sqrt{10}}{40}x$
$\Sigma_8{}^2P_A\frac{1}{2}^+$	0	0	0	0	$-\frac{3\sqrt{10}}{40}x$	0

$$\langle\phi_\Lambda^A|(\delta_{1s}+\delta_{2s})|\phi_\Lambda^\rho\rangle=\sqrt{2}/3\,, \tag{C7}$$

$$\langle\phi_\Lambda^\lambda|\delta_{1s}+\delta_{2s})|\phi_\Lambda^\lambda\rangle=1\,, \tag{C8}$$

$$\langle\phi_\Sigma^\lambda|(\delta_{1s}+\delta_{2s})|\phi_\Sigma^\lambda\rangle=\tfrac{1}{3}\,, \tag{C9}$$

$$\langle\phi_\Sigma^s|(\delta_{1s}+\delta_{2s})|\phi_\Sigma^s\rangle=\tfrac{2}{3}\,, \tag{C10}$$

$$\langle\phi_\Sigma^\lambda|(\delta_{1s}+\delta_{2s}|\phi_\Sigma^s\rangle=\sqrt{2}/3\,, \tag{C11}$$

these calculations then become straightforward. The resulting contact and tensor matrix elements in the SU(6) basis are given in Tables VIII and IX, respectively; the matrix elements in the *uds* basis may easily be obtained by using the formulas of Appendix B.

---

*Present and permanent address: Department of Physics, University of Toronto, Toronto, Canada M5S 1A7.

†Present and permanent address: Department of Physics, University of Guelph, Guelph, Canada N1G 2W1.

[1]N. Isgur and G. Karl, Phys. Lett. 72B, 109 (1977).

[2]N. Isgur and G. Karl, Phys. Lett. 74B, 353 (1978).

[3]N. Isgur and G. Karl, Phys. Rev. D 18, 4187 (1978).

[4]A. De Rújula, H. Georgi, and S. L. Glashow, Phys. Rev. D 12, 147 (1975).

[5]D. Gromes and I. O. Stamatescu, Nucl. Phys. B112, 213 (1976); W. Celmaster, Phys. Rev. D 15, 1391 (1977); D. Gromes, Nucl. Phys. B130, 18 (1977); L. J. Reinders, J. Phys. G 4, 1241 (1978).

[6]U. Elwanger, Nucl. Phys. B139, 422 (1978).

[7]H. J. Schnitzer, Phys. Lett. 65B, 239 (1976); 69B, 477 (1977); Phys. Rev. D 18, 3482 (1978); R. H. Graham and P. J. O'Donnell, *ibid.* 19, 284 (1979); B. R. Martin and L. J. Reinders, Nucl. Phys. B143, 309 (1978).

[8]A. B. Henriques, B. Kellett, and R. G. Moorhouse, Phys. Lett. 64B, 85 (1976); L. Him Chan, Phys. Lett. 71B, 422 (1977).

[9]R. Carlitz, S. D. Ellis, and R. Savit, Phys. Lett. 68B, 443 (1976); N. Isgur, Acta Phys. Polonica B8, 1081 (1977).

[10]G. Karl and E. Obryk, Nucl. Phys. B8, 809 (1968).

[11]W. P. Petersen and J. L. Rosner, Phys. Rev. D 6, 820 (1972); D. Faiman, *ibid.* 15, 854 (1977).

[12]This is the special case of an SU(6) rule appropriate to the potential model considered here. See R. H. Dalitz, in *Proceedings of the Triangle Meeting* (VEDA Publishing House, Bratislava, 1975), and R. Horgan and R. H. Dalitz, Nucl. Phys. B66, 135 (1973). This rule has also been noted in the case where $V^{ij}_{\rm conf}$ is a power-law potential by Gromes and Stamatescu (Ref. 5).

[13]G. Bunce *et al.*, Phys. Rev. Lett. 36, 1113 (1976).

[14]There is, however, a selection rule which forbids $^2\Sigma$ states with ρ-type wave functions (ρ in the P-wave baryons and $\rho\lambda$ in the positive-parity states) from decaying into $\Lambda\pi$.

[15]E. Pietarinen, in *Proceedings of the Topical Conference on Baryon Resonances, Oxford, 1976*, edited by R. T. Ross and D. H. Saxon (Rutherford Laboratory, Chilton, Didcot, England, 1977); R. E. Cutkosky, *ibid.*

[16]Particle Data Group, Phys. Lett. 75B, 1 (1978).

[17]B. R. Martin and M. K. Pidcock, Nucl. Phys. B127, 349 (1977).

[18]R. S. Langacre and J. Dolbeau, Nucl. Phys. B122, 493 (1977).

[19]D. Faiman, J. L. Rosner, and J. Weyers, Nucl. Phys. B57, 45 (1973); see also, however, Refs. 20 and 24.

[20]D. E. Novoseller, Nucl. Phys. B137, 445 (1978).

[21]G. P. Gopal *et al.*, Nucl. Phys. B119, 362 (1977); also Rev. 17.

[22]C. A. Heusch and R. Ravndal, Phys. Rev. Lett. 25, 253 (1970).

[23]J. Babcock *et al.*, Nucl. Phys. B126, 87 (1977).

[24]A. J. G. Hey, P. J. Litchfield, and R. J. Cashmore [Nucl. Phys. B95, 516 (1975)] have performed an $SU(6)_W$-type analysis of the positive-parity resonances that are candidates for the $(56,2^+)$ assuming they are not mixed with the $(70,2^+)$ and find reasonably good agreement. It is not clear, however, how mixing would have affected their results.

[25]In fact it was already mentioned in Ref. 3 that such effects may account for the deviation of $\Lambda(1405)\frac{1}{2}^-$ from its predicted position since it strongly couples to $\bar{K}N$ and it is near the $\bar{K}N$ threshold.

[26]R. R. Horgan, Nucl. Phys. B71, 514 (1974); M. Jones, R. H. Dalitz, and R. R. Horgan, *ibid.* B129, 45 (1977).